Studies on Cytotoxic Effects of Tumor Necrosis Factor-Related Apoptosis Inducing Ligand (TRAIL) to Canine Cell Lines Derived from Hemangiosarcoma and Mammary Epithelial Tumor

Studies on Cytotoxic Effects of Tumor Necrosis Factor-Related Apoptosis Inducing Ligand (TRAIL) to Canine Cell Lines Derived from Hemangiosarcoma and Mammary Epithelial Tumor

（犬の血管肉腫および乳腺上皮性腫瘍に由来する細胞株に対する腫瘍壊死因子関連アポトーシス誘導因子（TRAIL）の細胞傷害性に関する研究）

2019

The United Graduate School of Veterinary Sciences, Gifu University

(Gifu University)

GOTO, Minami

CONTENTS

PREFACE

In recent years, significant attention has been paid to various diseases occurring in companion animals due to improved awareness and the development of veterinary medicine. Among them, malignant tumors have a high incidence and mortality, and thus many veterinarians have made efforts to successfully resolve these challenges [5, 30, 39]. In addition, some malignant tumors in dogs and cats are attracting attention from the perspective of comparative oncology since they are not experimentally induced and are spontaneous tumors. They provide a possibility for spontaneous tumor models in research [39, 45, 58, 96]. Moreover, some malignant tumors are very rare in humans and are more frequently observed in dogs and cats. For example, hemangiosarcoma (HSA) is a malignant tumor frequently observed in dogs than in humans [60, 63, 114, 122]. Hence, the use of canine HSA is favorable to study HSA. Notably, new knowledge associated with HSA has been acquired from veterinary research [2, 3, 48, 49, 87]. Therefore, developing a tumor therapy useful in dogs is not only an important veterinary issue but can benefit research in the medical field.

On the other hand, specific malignant tumors observed in dogs and cats have different clinical and histological characteristics compared to their human counterparts, and hence their information cannot be applied to canine tumors [39, 45, 47, 59, 69, 74, 113, 146]. The canine mammary tumor (CMT) is an appropriate example representing this dilemma.

Canine HSA is the most frequent tumor in canine splenic tumors [56, 73].

This tumor is characterized by aggressive growth, early metastasis, resulting in poor prognosis especially in visceral HSA [60, 90, 116, 135]. In HSA, surgical excision is the first choice, but since surgery alone is less effective, adjuvant doxorubicin is administered [11]. In previous studies [35, 43, 79, 109], various drug combinations including metronomic therapy using low-dose cyclophosphamide with doxorubicin, have been evaluated in order to increase the effectiveness of these drugs. However, even with the use of these drugs, the survival time is 6 months or less [35, 43, 79]. Hence, it is necessary to understand the characteristics of canine HSA in order to establish a more effective treatment. Our laboratory has reported that vascular endothelial growth factor (VEGF), basic fibroblast growth factor (bFGF), their receptors (flt-1 and flk-1), and anti-apoptotic factors including survivin and Bcl-2 are highly expressed in spontaneous canine HSAs [86, 145]. Moreover, a xenograft model and canine HSA cell lines were established, allowing the dynamic assessment of canine HSA [64, 85]. Using these cell lines, it is now possible to evaluate the effects of medical drugs on canine HSA. To date, several studies have used canine HSA cell lines to evaluate the cytotoxic effect of drugs [4, 18, 29, 37].

CMT is an extremely common neoplasm in female dogs, with 20-80 % diagnosed as malignant [83]. Surgical excision is the first choice of treatment and adjuvant chemotherapy is required for cases with high-grade subtypes or lymphatic invasion of tumor cells, which indicates poor prognosis [76, 121]. In particular, lymphatic invasion and metastases to lymph nodes correlate with poor prognosis [42, 99, 128, 132]. Malignant subtype tumors, with invasion of dermal lymphatic vessels by neoplastic emboli and clinical signs of inflammation

are called inflammatory mammary carcinoma (IMC), which is the most aggressive and poor prognosis tumor in CMT [42, 76, 98]. IMC is severely painful, causes weakness and anorexia, and significantly reduces the quality of life [76, 98]. IMC is considered to be a poor surgical candidate owing to its poor prognosis, and the survival time is usually less than one month [98, 121]. In recent years, there have been reports suggesting that adjuvant chemotherapy may prolong survival time after surgical excision; however, no effective therapy has been established [76, 121]. Although the incidence of tumors defined as IMC is never high in CMT (about 18% of malignant CMT and 8% of all CMT), the development of effective chemotherapy is also crucial in other malignant mammary tumors with lymphatic invasion [98, 121]. Furthermore, besides comparing the effects of treatment methods in clinical cases, recent studies evaluating anti-tumor drugs in cell lines or xenograft models have been reported [24, 52, 78, 111, 130].

Recently, many new concept small-molecule compounds such as various tyrosine kinase inhibitors have been used in the treatment of systemic cancers in both human and veterinary medicine [16, 17, 19, 52, 78, 92, 120, 130]. These drugs target molecules characteristic of each tumor [16, 17, 19, 27, 33, 65, 92, 120]. Furthermore, anti-tumor cytokines, such as interleukin (IL), interferon (IFN), and tumor necrosis factor (TNF) α, which induce apoptosis or enhancement of immune system have also been investigated [36, 71, 82]. In particular, many studies have evaluated IL and IFN, with some clinical trials and applications [14, 36, 38, 81, 82, 127, 143]. In addition to these cytokines, TNF-related apoptosis-inducing ligand (TRAIL), also called Apo2 ligand (Apo2L),

was discovered as an anti-tumor cytokine belonging to the TNF protein family and has attracted attention [10, 142]. TRAIL is transcribed in many normal tissues, including the spleen, thymus, prostate, lung, and tonsillar T cells, as well as in several lymphoma cells such as Raji and K299 cells [142]. TRAIL is reported to induce apoptosis in several tumor cells but not in normal cells [10, 101, 138, 142]. There are two main signaling pathways that induce apoptosis: the intrinsic pathway and the extrinsic pathway [129]. The intrinsic pathway is mainly initiated in the mitochondria and is mediated by p53 as a result of DNA damage [129, 140, 141]. Notably, p53 regulates Bax, Apaf-1, and other apoptosis-related molecules [137, 140]. Bax and Bak induce cytochrome c release from the mitochondria and released cytochrome c forms apoptosomes with Apaf-1 and caspase-9, subsequently activating caspase-3 [23, 89, 141]. Thus, p53 has an important role in the apoptosis-inducing pathway and is the most commonly silenced or mutated gene in most cancers, with 50–55% of all human cancers characterized by loss of wild-type p53 activity [140]. Additionally, the intrinsic pathway is activated by caspase-8 which cleaves Bid, and the cleaved Bid (tBid) activates Bax and Bak [22, 89]. In the extrinsic pathway, the death receptor (DR) on the cell surface activates caspase-8 via FADD, and this initiator caspase activates caspase-3 directly [89, 129]. The cells are classified into two types based on the cellular response after caspase-8 activation: type-I cells mainly activate the extrinsic pathway and type-II cells rely on the intrinsic pathway [89, 129]. TRAIL activates caspase-8, resulting in the activation of both extrinsic and intrinsic pathways in a p53-independent or dependent manner, and is expected to exhibit a broad anti-tumor effect even in tumor cells carrying a p53 mutation

[22, 89]. Additionally, some studies have reported that TRAIL exhibits anti-tumor effects without marked systemic side effects in the mouse xenotransplantation model and cynomolgus monkeys [10, 54, 57]. Therefore, in human medicine, TRAIL is anticipated to be an effective new therapy in neoplastic diseases. Besides simply administering TRAIL, another treatment strategy has been studied to activate its signaling pathway, which can be achieved with anti-TRAIL receptor agonist or a small-molecule compound [TRAIL-inducing compound 10 (TIC10)] to induce intrinsic TRAIL production *in vivo* [7, 9, 46, 89, 142]. In addition, studies on the mechanism underlying TRAIL resistance in cancer cells are ongoing [89, 134]. Accordingly, various strategies for the effective activation of the TRAIL pathway can be selected.

In veterinary medicine, the effect of TRAIL has been evaluated in canine mast cell tumors, canine osteosarcoma cell lines, lymphoma cell lines, and mammary tumor cell lines [31, 97, 110, 123]; however, knowledge regarding the TRAIL mechanism of action in canine tumor cells is insufficient. In humans, experiments using several tumor cell lines have been conducted to clarify the mechanism of action of TRAIL and the mechanism of acquired resistance [134, 148]. On the other hand, only two studies have reported the anti-tumor effect of TRAIL after a single administration and the knowledge regarding TRAIL is too scarce for further research in veterinary medicine [31, 110]. The purpose of this study was to evaluate the effects of TRAIL on canine tumor cells and generate basic information that is necessary for further research on the mechanism of TRAIL action and acquiring TRAIL resistance.

In chapter 1 of this study, the cytotoxic effect of human recombinant

TRAIL (rhTRAIL) on canine HSA cell lines was investigated. In chapter 2, three new cell lines were cultured from CMT, and the cytotoxic effect of rhTRAIL on these three new cell lines was evaluated.

Chapter 1

The cytotoxic effect of TRAIL to canine hemangiosarcoma cell lines

1.1 INTRODUCTION

Canine HSA is a malignant tumor that mainly occurs in the spleen, subcutaneous tissue, and in the right atrium of the heart [13, 116, 135]. HSAs are extremely aggressive tumors, exhibiting metastasis and invasive growth, contributing to a very poor prognosis, especially in case of visceral HSAs [103, 116, 122, 135]. Previous studies have demonstrated an association of several factors with the malignant behavior and tumorigenesis of canine HSA, such as the enhanced expression of VEGF and bFGF, mutations of several oncogenes, and activation of various signaling pathways [28, 60, 85, 144, 145].

Despite continuous progress in elucidating the oncogenic mechanism of canine HSA, along with the identification of potential therapeutic targets, no effective therapeutic strategy has been identified. The survival time following splenectomy in dogs with splenic HSA is extremely short; even when splenectomy and chemotherapy are used in combination, the survival time is only about 6 months [13, 35, 43, 103]. One of the main contributing factors to this poor prognosis is the high rate of metastasis in canine HSA. Hence, a systemic therapy targeting the metastatic lesions and the original tumor need to be developed. TRAIL is one such candidate, specifically acting on tumor cells and not on normal cells. However, the effects of TRAIL, an anti-tumor cytokine, on HSAs have not yet been reported in human or veterinary medicine. Therefore, the aim of this chapter was to clarify the cytotoxic effects of TRAIL in canine

HSA and provide a scientific foundation for the potential effectiveness of TRAIL in the treatment of canine tumors. The effects of TRAIL in various HSA cell lines were explored to provide basic information on the TRAIL sensitivity of canine HSA cells.

1.2 MATERIALS AND METHODS

Cells and culture conditions

Canine HSA cell lines established from the liver (JuA1, JuB2, JuB2-1, and JuB4), right atrium of the heart (Re11, Re12, and Re21), and spleen (Ud2 and Ud6) were used in this study [64, 85]. Madin-Darby canine kidney (MDCK, resistant to TRAIL) and HeLa cells (sensitive to TRAIL) were used as negative and positive controls, respectively (both from the JCRB Cell Bank, Osaka, Japan) [31, 101, 110]. Canine aortic endothelial cells (CnAOECs; Cell Applications Inc., San Diego, CA, USA) were used as a normal canine vascular endothelial cell line to evaluate the cytotoxicity of TRAIL against normal cells. The HSA cell lines, MDCK cells, and HeLa cells were maintained in high-glucose Dulbecco's modified Eagle medium (Wako Pure Chemicals, Osaka, Japan) with 10% heat-inactivated fetal bovine serum (FBS), 100 units/m*l* penicillin, 100 μg/m*l* streptomycin, 0.25 μg/m*l* amphotericin B (Penicillin-Streptomycin-Amphotericin B Suspension, Wako Pure Chemicals), and 100 μg/m*l* kanamycin (Wako Pure Chemicals) (10% FBS/D-MEM). CnAOEC cells were maintained in Canine Endothelial Cell Growth Medium (Cell Applications Inc.). All cells were incubated at 100% humidity, 37°C, with 20% O_2 and 5% CO_2.

TRAILs

In this study, the cytotoxicity and apoptosis induction ability of the three TRAILs were assessed: rhTRAIL/TNFSF10 375-TEC (TRAIL-TEC, R&D Systems, Minneapolis, MN, USA), rhTRAIL/TNFSF10 375-TL (TRAIL-TL, R&D

Systems), and isoleucine zipper rhTRAIL (izTRAIL, AdipoGen Life Sciences Inc., San Diego, CA, USA). TRAIL-TEC (amino acids 114Thr-281Gly) was expressed in *Escherichia coli*, TRAIL-TL (amino acids 95Thr-281Gly) was expressed in the NSO mouse myeloma cell line, and izTRAIL (amino acids 95Thr-281Gly) was expressed in *E. coli*.

Cell viability assay

Cell viability assays were performed with the premix WST-1 cell proliferation assay system (TaKaRa, Otsu, Japan). HSA and HeLa cells were seeded in 96-well plates at a density of 1.0×10^4 cells per well. MDCK cells were seeded at a density of 2.5×10^3 cells per well due to their relatively fast proliferation rate. After 12 h, the cells were treated with 10% FBS/D-MEM containing 0, 0.01, 0.1, 1.0, 10, or 100 ng/m*l* of TRAIL-TEC, TRAIL-TL, or izTRAIL for 24, 48, and 72 h. Following treatment, the cells were incubated with 10 μ*l* of WST-1 reagent per well for 1 h. Cell viability was then quantified using the iMark™ microplate reader (Bio-Rad Laboratories, Hercules, CA, USA) as the relative absorbance value obtained in the treated wells compared to the control (0 ng/m*l* TRAIL) wells. The half-maximal inhibitory concentration (IC_{50}) of each TRAIL was calculated by Image J 1.51K (National Institutes of Health, Bethesda, MD, USA) based on the results of the viability assay.

The effect of izTRAIL (which had the most potent cytotoxic effect) on CnAOEC viability was also evaluated. CnAOECs were seeded in 96-well plates at a density of 1.0×10^4 cells per well. After 12 h, the cells were treated with Canine Endothelial Cell Growth Medium containing 0, 0.01, 0.1, 1.0, 10, and 100

ng/m*l* of izTRAIL for 24, 48, and 72 h. Measurement of cell viability and calculation of IC_{50} values was performed as described above.

Flow cytometric analysis of apoptosis

JuB4 and Ud6 cells were identified to be the most sensitive cell lines to TRAIL for each lineage and were thus selected for further analysis of apoptosis induction. Since Re12 and Re21 cells demonstrated similar susceptibility to TRAIL, only Re12 was used for further analysis. JuB4, Re12, and Ud6 cells were treated with 100 ng/m*l* izTRAIL, and apoptosis was detected using flow cytometry after 4, 8, 12, 24, and 36 h, corresponding to the time periods before cell viability significantly decreased. The cells were collected with 0.25% Trypsin-1 mM EDTA・4Na solution (T/E solution, Wako Pure Chemicals), washed with Dulbecco's phosphate-buffered saline (D-PBS, Wako Pure Chemicals), and stained with Annexin V/ propidium iodide (PI) (Alexa Fluor 488 Annexin V/Dead cell Apoptosis Kit, ThermoFisher Scientific, Waltham, MA, USA). The cells were counted using FACS Calibur (BD Biosciences, Franklin Lakes, NJ, USA) and analyzed by BD CellQuest Pro ver. 5.1.1 (BD Biosciences).

For analysis of the cell cycle, JuB4, Re12, and Ud6 were treated with 100 ng/m*l* izTRAIL for 48 h (the point at which cell viability significantly decreased), the supernatant and cells were collected with T/E solution and washed with D-PBS. The collected cells were then incubated with PI (PI/RNase staining solution, Cell Signaling Technology, Danvers, MA, USA). Stained cells were counted by BD FACSCanto™Ⅱ(BD Biosciences) and analyzed by BD FACSDiva 6.1 software (BD Biosciences).

Observations of nuclear fragmentation

JuB4, Re12, Ud6, and MDCK cells were cultured at 2.0×10^5cells per well in a chamber slide for 12 h to observe the effect of TRAIL on nuclear fragmentation using fluorescence microscopy. The cells were treated with 100 ng/m*l* izTRAIL for 36 h, and then washed with D-PBS, and fixed in 4% paraformaldehyde (Wako Pure Chemicals) for 30 min. The slides were washed with D-PBS, mounted with ProLong™ Diamond antifade Mountant with 4',6-diamidino-2-phenylindole (DAPI) nuclear stain (ThermoFisher Scientific), and the presence of DNA fragmentation was assessed using fluorescence microscopy (IX73, Olympus, Tokyo, Japan).

Sodium dodecyl sulfate-polyacrylamide gel electrophoresis (SDS-PAGE)

To detect the effects of TRAIL on apoptosis-related proteins, JuB4, Re12, and Ud6 cells were collected using a cell scraper at 1, 3, 6, 12, and 24 h after treatment with 100 ng/m*l* izTRAIL. The cells were then lysed using RIPA buffer (ThermoFisher Scientific) containing proteinase inhibitor cocktail and EDTA (ThermoFisher Scientific). The concentration of the extracted protein was measured by the DC Protein assay kit (Bio-Rad), and standardized using serially diluted bovine serum albumin (ThermoFisher Scientific).

The equalized protein samples were mixed with 4× Laemmli buffer (Bio-Rad) supplemented with 5% ß-mercaptoethanol (Sigma Aldrich, St. Louis, MO, USA) and incubated at 95°C for 10 min. Proteins (15 μg/lane) were then separated by SDS-PAGE (4–12.5% Mini-PROTEAN® TGX™ Precast Protein Gels, Bio-Rad) and transferred onto a polyvinylidene difluoride (PVDF) membrane

(Amersham Hybond P0.45 PVDF, GE Healthcare Bioscience, Pittsburgh, PA, USA) at 60 V for 1.5 h at room temperature (20-25 °C: RT).

Western blotting

The membranes, with transferred proteins, were immersed in 5% blocking reagent (ThermoFisher Scientific) for 1 h at RT, followed by incubation with primary goat polyclonal anti-caspase-8 (1: 800, T-16, Santa Cruz Biotechnology, Dallas, TX, USA), rabbit polyclonal anti-caspase-3 (1:1000, Cell Signaling Technology), rabbit polyclonal anti-Poly (ADP-ribose) polymerase (PARP, 1:1000, ThermoFisher Scientific), or ß-actin (1:1000, Cell Signaling Technology) for 1 h at RT. The primary antibodies were used after confirming the reaction with proteins of the same size as indicated in the previous study for both the HeLa cells and canine HSA cells [49, 112].

The membranes were washed with TBS-T (0.05 M Tris, 0.138 M NaCl, 0.0027 M KCl, and 0.05% Tween 20; Sigma Aldrich) and incubated with the appropriate horseradish peroxidase (HRP)-conjugated secondary antibody (anti-rabbit, 1:5000, Cell Signaling Technology or anti-goat, 1:2000, Abcam, Cambridge, UK) for 1 h at RT. The immunoblot was visualized using Lumina Forte Western HRP Substrate (Merck Millipore, Darmstadt, Germany). The target protein bands were visualized by the C-DiGit Blot scanner (LI-COR Biotechnology, Lincoln, NE, USA), and Image Studio Digits ver4.0 (LI-COR Biotechnology) and were verified semi-quantitatively relative to the expression of ß-actin.

Inhibition of caspase-8 or caspase-3

To determine the involvement of the caspase cascade in TRAIL-induced apoptosis, all HSA cell lines seeded in 96-well plates were treated with 0, 2.5, 10, and 40 μM of a caspase-8 inhibitor (Z-IETD-FMK, MBL, Nagoya, Japan) or caspase-3 inhibitor (Z-DEVD-FMK, MBL) for 2 h. Both caspase inhibitors were dissolved in dimethyl sulfoxide (DMSO). Subsequently, the cells were incubated with 100 ng/m*l* izTRAIL for 24 and 48 h, and the WST-1 assay was performed as described above. JuB4, Re12, and Ud6 cells were treated with caspase-8 and -3 inhibitors before the addition of izTRAIL, the attached and suspended cells were collected and stained with PI/RNase staining solution (Cell Signaling Technology), and cell cycle analysis was performed by flow cytometry.

Statistical analysis

All experiments were performed more than three times independently. Cell viability assay results were statistically evaluated by one-way analysis of variance and the Dunnet's posthoc test. The percentage of Annexin V positive and PI negative (Annexin V+/PI-) cells (i.e., apoptotic cells) or cells in the sub-G1 phase were compared between groups using the Student's t-test. These tests were performed by BellCurve for Excel (Social Survey Research Information Co., Ltd, Tokyo, Japan). All values are expressed as mean ± standard deviation (SD). Results were considered significant when $P < 0.05$.

1.3 RESULTS

Cell viability and IC_{50} of TRAILs

Despite minimal changes in the relative absorbance values of canine HSA cells, MDCK cells, and HeLa cells at specific time points after treatment with up to 100 ng/m*l* TRAIL-TEC, no significant decrease in cell viability was observed up to 72 h (Fig.1-1).

However, 100 ng/m*l* TRAIL-TL significantly decreased the cell viability of JuB2, JuB2-1, JuB4, Re12, and HeLa cells after 24, 48, and 72 h. In Re21 cells, 1, 10, and 100 ng/m*l* of TRAIL-TL decreased the cell viability after 72 h. However, no reproducible and significant cytotoxic effects of TRAIL-TL were observed in the other cell lines up to 100 ng/m*l* at any time points (Fig. 1-2).

Notably, izTRAIL decreased cell viability in all canine HSA cells except for Re11, and in HeLa cells in time- and concentration-dependent manners (Fig. 1-3). However, izTRAIL did not demonstrate a significant cytotoxic effect on MDCK or CnAOEC endothelial cells (Fig. 1-3). The IC_{50} values of izTRAIL 72 h after treatment are summarized in Table 1-1; however, the IC_{50} values could not be estimated for TRAIL-TEC due to the overall weak cytotoxic effect. In TRIAL-TL, IC_{50} could only be calculated with JuB2-1 (90.92±0.90) and JuB4 (13.09±0.46). The IC_{50} values of izTRAIL to HeLa cells were similar. Overall, JuB4 cells were the most sensitive cell line to izTRAIL.

Effects of izTRAIL on cell morphology and apoptosis induction

Since izTRAIL demonstrated the most potent cytotoxic effect on cancer cells with no influence on the viability of normal cells, its cancer cell inhibitory

mechanism through apoptosis was evaluated. After treatment with 100 ng/m*l* izTRAIL for 36 h, JuB4, Re12, and Ud6 cells indicated a clear detachment from the dishes and the number of cells decreased (Fig. 1-4A). Flow cytometric analysis further demonstrated an increase in the cell number in the gray area, representing Annexin V+/PI- apoptotic cells, 36 h after izTRAIL treatment in JuB4, Re12, and Ud6 (Fig. 1-4B), demonstrating statistical significance in all the three cell lines (Fig.1- 4C). In contrast, MDCK cells remained tightly attached as a monolayer to the dish, with no morphological changes observed after izTRAIL treatment (Fig. 1-4A).

DAPI staining further revealed nuclear fragmentation in JuB4, Re12, and Ud6 cells 36 h after treatment with 100 ng/m*l* izTRAIL (Fig. 1-5A), whereas MDCK cells displayed no nuclear fragmentation after 36 h with identical treatment. Cell cycle analysis revealed a marked increase in cells in the sub-G1 phase and a corresponding decrease in G0/G1-phase cells in the JuB4, Re12, and Ud6 cell lines 48 h after treatment with 100 ng/m*l* izTRAIL (Fig. 1-5B and C).

Western blotting for caspase-8, cleaved caspase-3, and PARP

Caspase-8, caspase-3, and PARP were detected by western blotting in JuB4, Re12, and Ud6 cells after treatment with izTRAIL; however, the time points at which these proteins were detected differed among the cell lines (Fig. 1-6). In JuB4 cells, cleaved caspase-8 expression increased 1–24 h after treatment, cleaved caspase-3 increased from 1 h after treatment, and cleaved PARP increased 1–24 h after treatment. In Re12 cells, cleaved caspase-8 increased 3–24 h after treatment and cleaved caspase-3 increased from 1 h after

treatment. Cleaved PARP was minimally increased 3–24 h after treatment and uncleaved PARP decreased from 3 h after treatment. In Ud6 cells, cleaved caspase-8, cleaved caspase-3 and cleaved PARP increased at 3–24 h after treatment.

Caspase-8 and caspase-3 inhibitors prevented TRAIL-induced apoptosis in canine HSA cells

The WST-1 assays demonstrated that both caspase inhibitors recovered the TRAIL-induced loss of cell viability at 40 μM in all HSA cell lines and in HeLa cells (Fig.1-7A). The caspase-3 inhibitor was more effective in preserving cell viability under izTRAIL treatment than the caspase-8 inhibitor in JuA1, JuB2, JuB2-1, and JuB4 cells. Furthermore, the flow cytometry results indicated that caspase-8 and caspase-3 inhibitors decreased the numbers of cells in the sub-G1 phase and increased the numbers of cells in the G0/G1 phase (Fig. 1-7B). The number of cells in the sub-G1 phase significantly decreased in JuB4 and Ud6 cells after the addition of the caspase-3 inhibitor. Consistently, although not statistically significant, a decrease in the number of sub-G1 phase cells was observed in the Re12 cells (Fig.1-7C).

1.4 DISCUSSION

The cytotoxic effects of the three types of rhTRAILs were evaluated. The human and dog TRAIL sequence identity is 81.3%, and the amino acid sequences of the trimeric or receptor- binding domains of TRAIL are highly conserved [102, 110]. A previous study demonstrated that rhTRAIL, the same as TRAIL-TEC used in this study, induced apoptosis in a canine mast cell tumor cell line [31]. Of the three rhTRAIL proteins examined, izTRAIL demonstrated the strongest ability to induce apoptosis in canine HSA cells. Based on a previous report, it is likely that the TRAIL trimer formed via the zipper motifs as observed in izTRAIL could be more stable than the monomeric form, and thus more effective against neoplastic cells [138]. TRAIL-TL has a His-Tag at the N-terminal region, able to bind to the zinc ion necessary for TRAIL trimerization; thus, the formation of a TRAIL-TL trimer is more probable than the formation of a TRAIL-TEC trimer, which has no His-tags [53, 75, 126]. Therefore, TRAIL-TEC may also affect HSA cell lines at higher concentrations than tested in this study.

In medical research, it has been reported that TRAIL activates caspase-8, leading to the activation of both extrinsic and intrinsic pathways in a p53-independent or dependent manner [22, 89]. In the Re12 and Ud6 canine HSA cell lines used in this study, p53 activity was reported to be decreased by downregulation of miR-214 and COP1 E3 ubiquitin-protein ligase overexpression [49]. Therefore, the present study demonstrated that TRAIL can induce Re12 and Ud6 apoptosis, indicating the apoptosis-inducing effect in neoplastic cells of canine HSA in which p53 is inactivated. In addition to these two tumors, *p53* mutations have been reported in several canine tumors [55, 67, 80, 88, 136].

TRAIL may be effective in these tumors with p53 inactivation.

Five TRAIL receptor variants have been identified in humans [26, 32, 70, 77, 94, 95, 115, 118, 139]. Of these receptors, only DR 4 and DR5 have the death domains necessary for the induction of apoptosis, while the other receptors such as decoy receptor (DcR)1, DcR2, and osteoprotegerin (OPG) present no region capable of transmitting a signal into the cell [26, 32, 70, 77, 94, 95, 115, 139] Previous studies have indicated that when TRAIL binds to DR4 or DR5, it activates the Fas-associated death domain (FADD) protein and induces apoptosis through the activation of caspase-8/10 and caspase-3 [61, 70, 124]. Moreover, DcRs are expressed in normal cells; however, the balance of expression of each receptor differs from that observed in neoplastic cells [66]. Therefore, many normal cells are resistant to apoptosis induced by TRAIL. In veterinary medicine, the effect of TRAIL in canine mast cell tumor cell lines revealed a role for the activation of caspase-3 [31]. In addition, caspase-8 was activated by flavopiridol (FVP) in lymphoma cell lines exhibiting TRAIL resistance, but it remains unclear whether TRAIL also activated caspase-8 [97]. At present, the only TRAIL receptor identified in dogs is OPG, and its transfer signals have only recently been predicted based on gene sequence analysis [31, 40]. Therefore, how TRAIL receptors act in canine tumor cell lines and the mechanism of action of TRAIL remains unclear. In this study, all cell lines used in the western blot analysis were found to express cleaved PARP, with the activation of caspase-8 and caspase-3 under TRAIL treatment. In addition, the clear inhibition of apoptosis, but not the complete inhibition, following treatment with caspase-8 and caspase-3 inhibitors, in all cell lines, suggests that caspase-8 and caspase-3 are

at least partially involved in TRAIL-induced apoptosis. One possible reason for the greater effectiveness of the caspase-3 inhibitor in the Ju cell lineage could be attributed to the compensatory activation of caspase-10, which performs the same role as caspase-8, or to a small amount of cleaved caspase-8 continuously activating caspase-3, which has been reported in various cascade reactions [6, 62]. Alternatively, in the Re and Ud lineages, caspase-8 may be inhibited by several factors before activating caspase-3. In addition to directly activating caspase-3, caspase-8 can activate caspase-3 via caspase-9 [104]. Moreover, Bcl-2 has been reported to be overexpressed in canine HSA [86]. When Bcl-2 is expressed, activation of caspase-3 via caspase-9 is suppressed, and caspase-8 remains the only direct activator of caspase-3 [148]. This inhibition of caspase-3 is consistent with the lower IC_{50} values demonstrated by the Ju cells compared to the other cell lines; however, further evaluation of the Bcl-2 expression levels in HSA cell lines is crucial to verify this hypothesis.

Several studies have reported that neoplastic cells expressing DcRs show resistance to TRAIL [25, 117, 148]. However, other reports have also suggested that other factors could contribute to TRAIL resistance, including anti-apoptotic factors such as Bcl-2 and c-FLIP [44, 91, 148]. Moreover, survivin expression has also been confirmed in canine HSA, which belongs to the same IAP family as the X-linked inhibitor of apoptosis (XIAP) shown to be related to TRAIL resistance in canine mammary cell tumors and osteosarcoma [86, 123]. Thus, the difference in expression of anti-apoptotic molecules in canine HSA is considered to contribute to the difference in TRAIL sensitivity among the lineages evaluated in this study. TRAIL sensitivity may be increased by the

inhibition of some anti-apoptotic factors such as Bcl-2, survivin, or XIAP, related to the apoptosis pathway via caspase-9 [86, 123]. Inhibition of c-FLIP, which allows the activation of caspase-8, has also been reported in canine lymphoma cells; however, since activation of caspase-8 with TRAIL treatment was detected, it is considered that c-FLIP does not influence the apoptosis mechanism [97, 148]. To explore the application potential of TRAIL to a wider range of canine tumors, it is necessary to study the factors related to the acquisition of TRAIL resistance, including DcRs and anti-apoptotic factors. It is expected that TRAIL may be widely applied in TRAIL-resistant canine tumors in combination with FVP inhibiting c-FLIP or TIC10, which also increases TRAIL DR expression [46, 97].

1.5 SUMMARY

A clear cytotoxic effect of TRAIL in canine HSA cell lines was demonstrated, with no cytotoxicity detected in normal canine endothelial cells. Since the degree of decreased cell viability varies depending on the three types of TRAIL, it was reported that the trimer form of TRAIL was more effective than the TRAIL monomer. The cytotoxicity of TRAIL was confirmed to be due to apoptosis as a result of cell membrane changes, nuclear fragmentation, caspase-8 and -3 activation, and PAPR cleavage. These results further suggest that this apoptosis induction at least partially involves caspase-8 associated with DR.

TABLE AND FIGURES

Table1-1. IC_{50} of canine HSA cell lines for izTRAIL

cells	izTRAIL (ng/ml)
JuA1	12.40 ± 8.11
JuB2	3.40 ± 2.75
JuB2-1	4.59 ± 5.56
JuB4	1.22 ± 0.46
Re11	-
Re12	11.57 ± 6.75
Re21	14.18 ± 3.53
Ud2	9.21 ± 6.98
Ud6	9.68 ± 5.00
MDCK	-
HeLa	12.65 ± 9.64

IC_{50} values of izTRAIL in canine HSA cell lines. Results are presented as mean ± SD of three independent experiments. －, cases in which the IC_{50} could not be calculated.

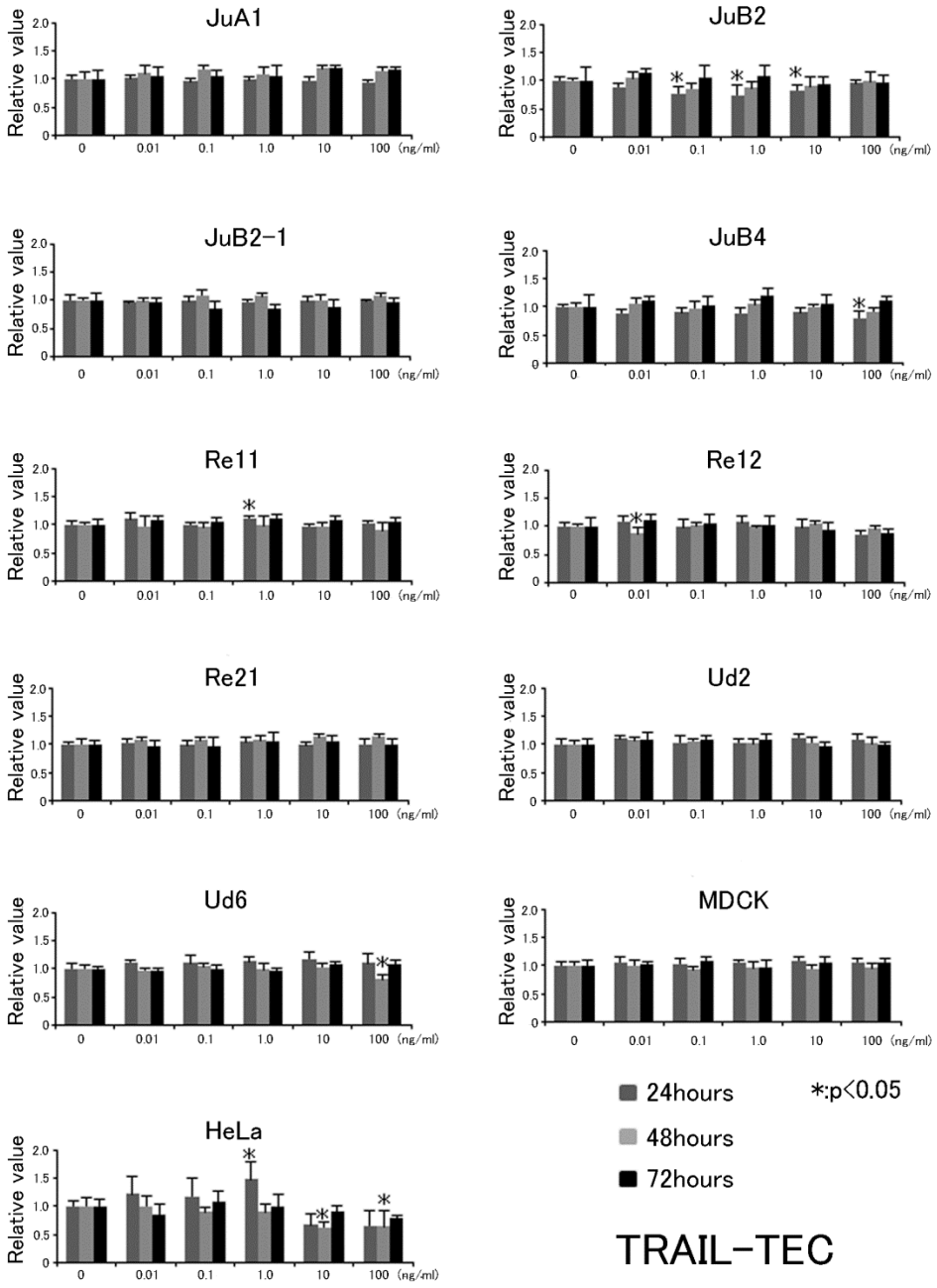

Fig. 1-1. Cell viability of canine HSA cell lines, MDCK cells, and HeLa cells after TRAIL-TEC treatment. The vertical axis shows the relative absorbance value compared with that of the control group (no TRAIL-TEC treatment) and the horizontal axis shows the concentration of TRAIL-TEC. Representative results of more than three independent experiments are presented as the mean ± SD (*P < 0.05).

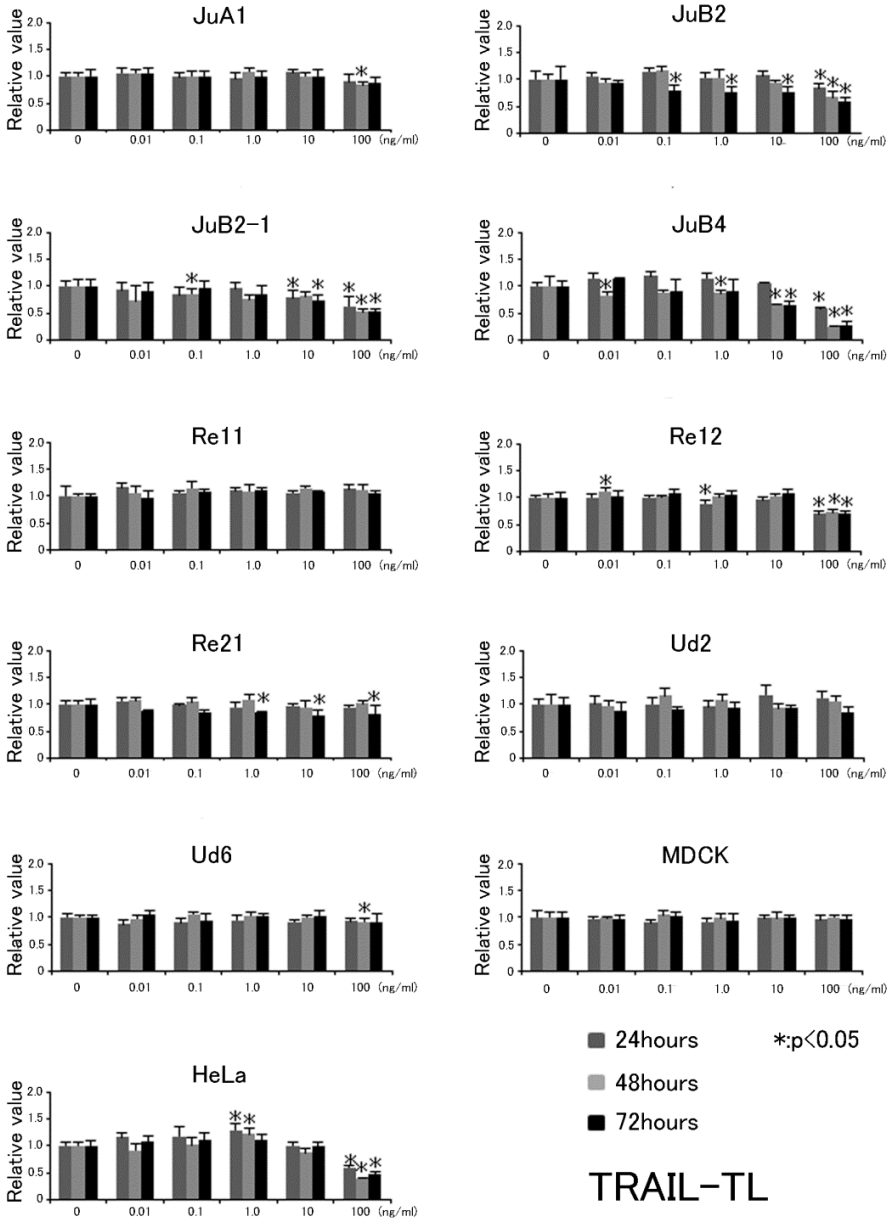

Fig. 1-2. Cell viability of canine HSA cell lines, MDCK cells, and HeLa cells after TRAIL-TL treatment. The vertical axis shows the relative absorbance value compared with the control group (no TRAIL-TL treatment) and the horizontal axis shows the concentration of TRAIL-TL. Representative results of more than three independent experiments are presented as the mean ± SD (*P < 0.05).

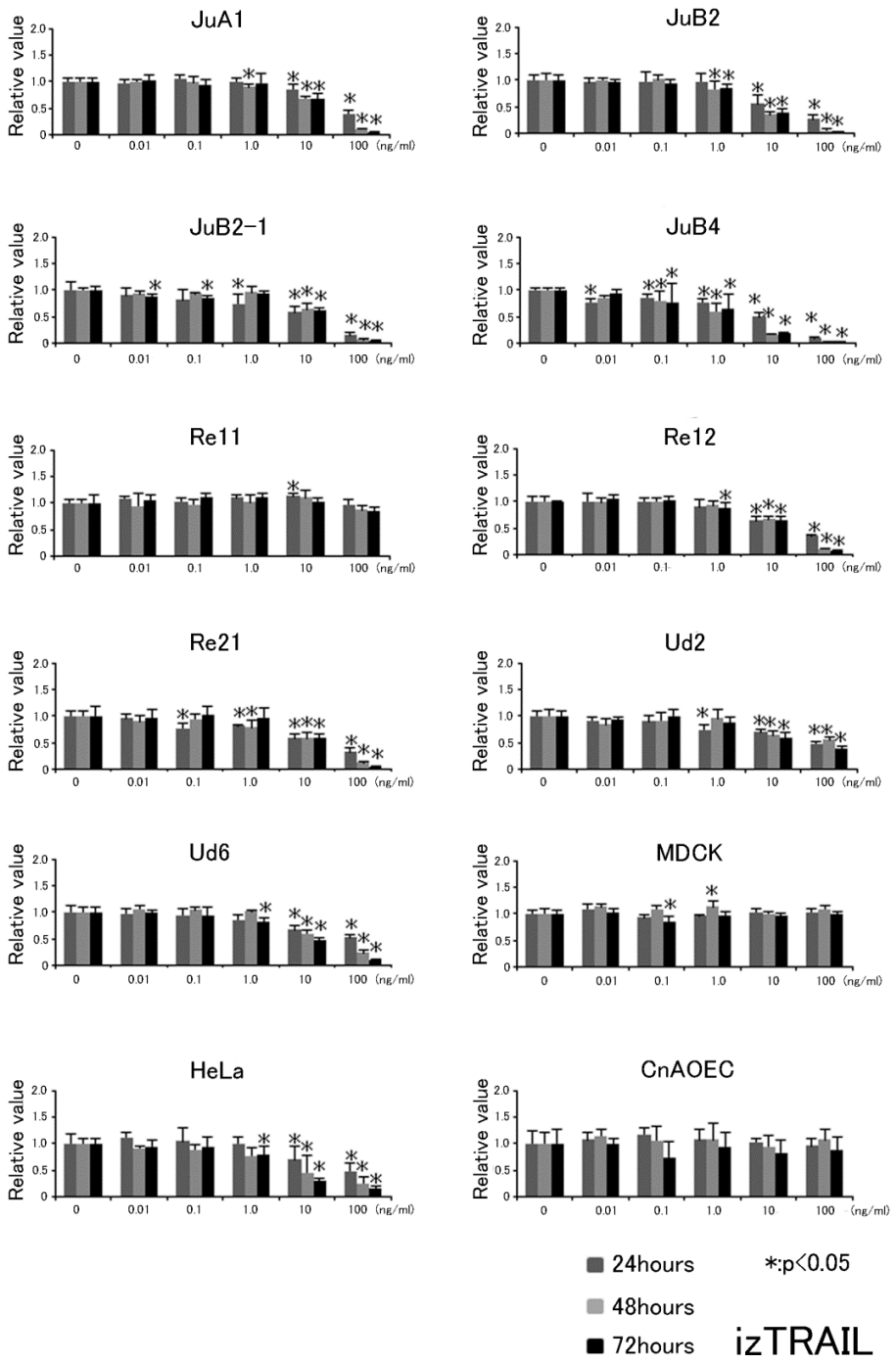

Fig. 1-3. Cell viability of canine HSA cell lines, MDCK cells, HeLa cells, and CnAOECs after izTRAIL treatment. The vertical axis shows the relative absorbance value compared with the control group (no izTRAIL treatment) and the horizontal axis shows the concentration of izTRAIL. Representative results of more than three independent experiments are presented as the mean ± SD (*P < 0.05).

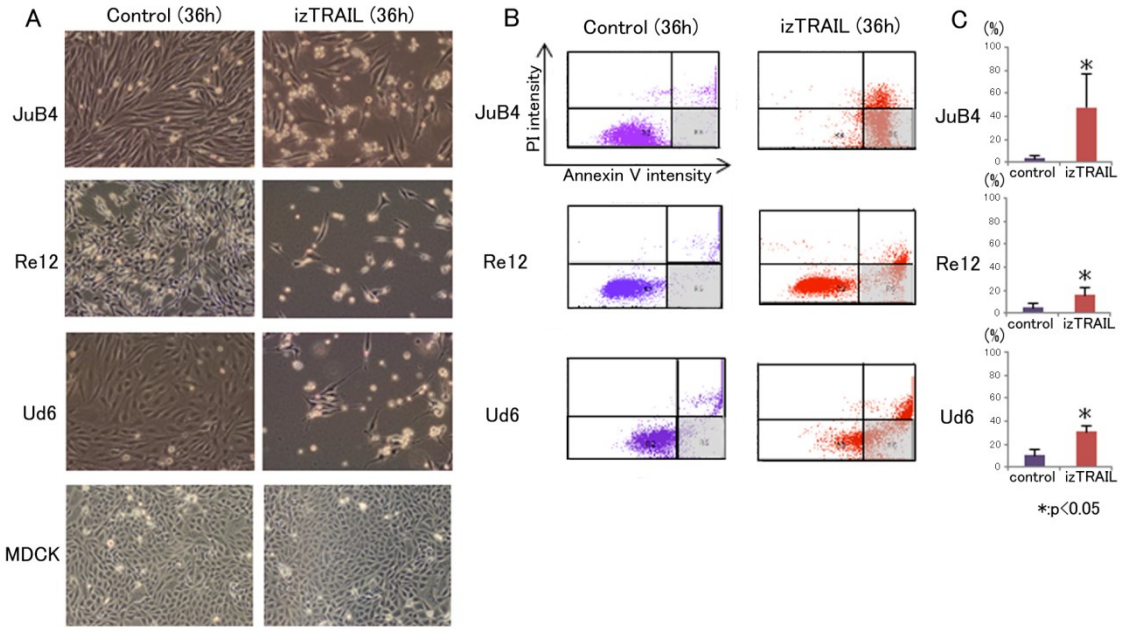

Fig. 1-4. Changes in cell morphology and percentage of Annexin V+/PI- cells after incubation with izTRAIL. A: In JuB4, Re12, Ud6 and MDCK cells treated with 100 ng/m*l* of izTRAIL for 36 h, the proportion of cell number decreased. B: Cells of each cell line stained with Annexin V/ PI. The vertical axis shows the PI staining intensity and the horizontal axis shows the Annexin V staining intensity. The cells in the gray area are Annexin V+/PI- (apoptotic cells). C: Mean percentage of Annexin V+/PI- cells (cells in the gray area of B) from replicate experiments. The Annexin V+/PI- cells increased significantly (*P < 0.05) in JuB4, Re12 and Ud6 cell lines.

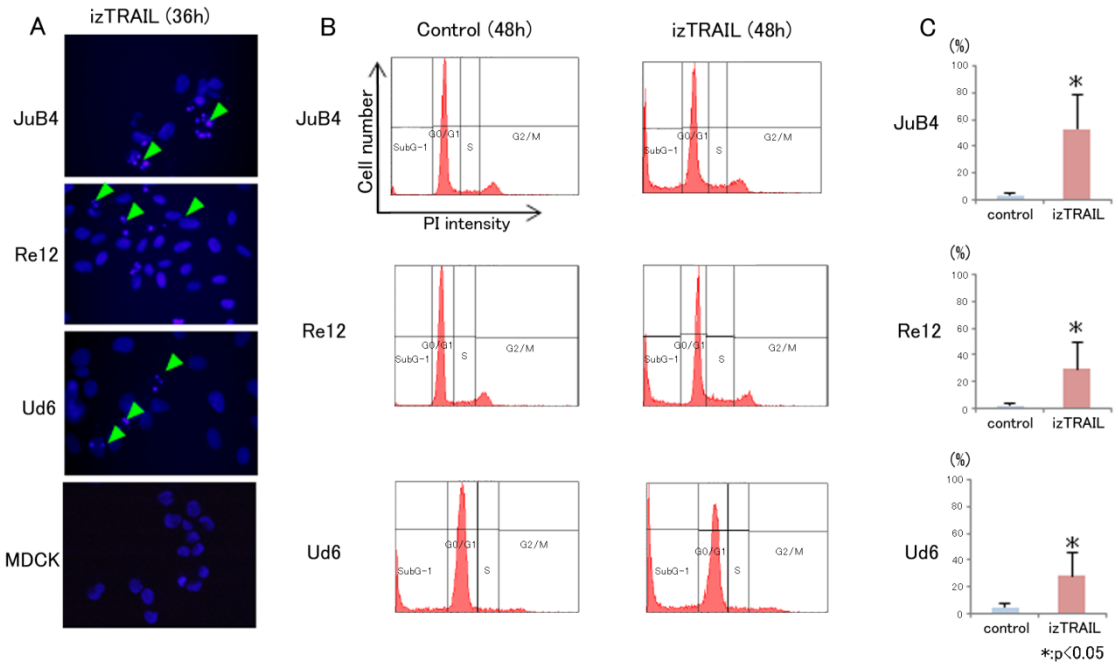

Fig. 1-5. Nuclear fragmentation induced by izTRAIL. A: DAPI staining revealed the nuclear morphology changes in JuB4, Re12, Ud6, and MDCK cells treated with 100 ng/m*l* of izTRAIL for 36 h. Arrowheads show the nuclear fragments. B: Representative DNA histogram showing the cells stained by PI for each cell line. JuB4, Re12, and Ud6 cells were treated with izTRAIL for 48 h and stained with PI. The vertical axis shows the cell number and the horizontal axis shows the PI staining intensity. C: The percentage of cells in sub-G1 phase increased significantly for JuB4, Re12, and Ud6 cell lines after treatment with izTRAIL (*P < 0.05).

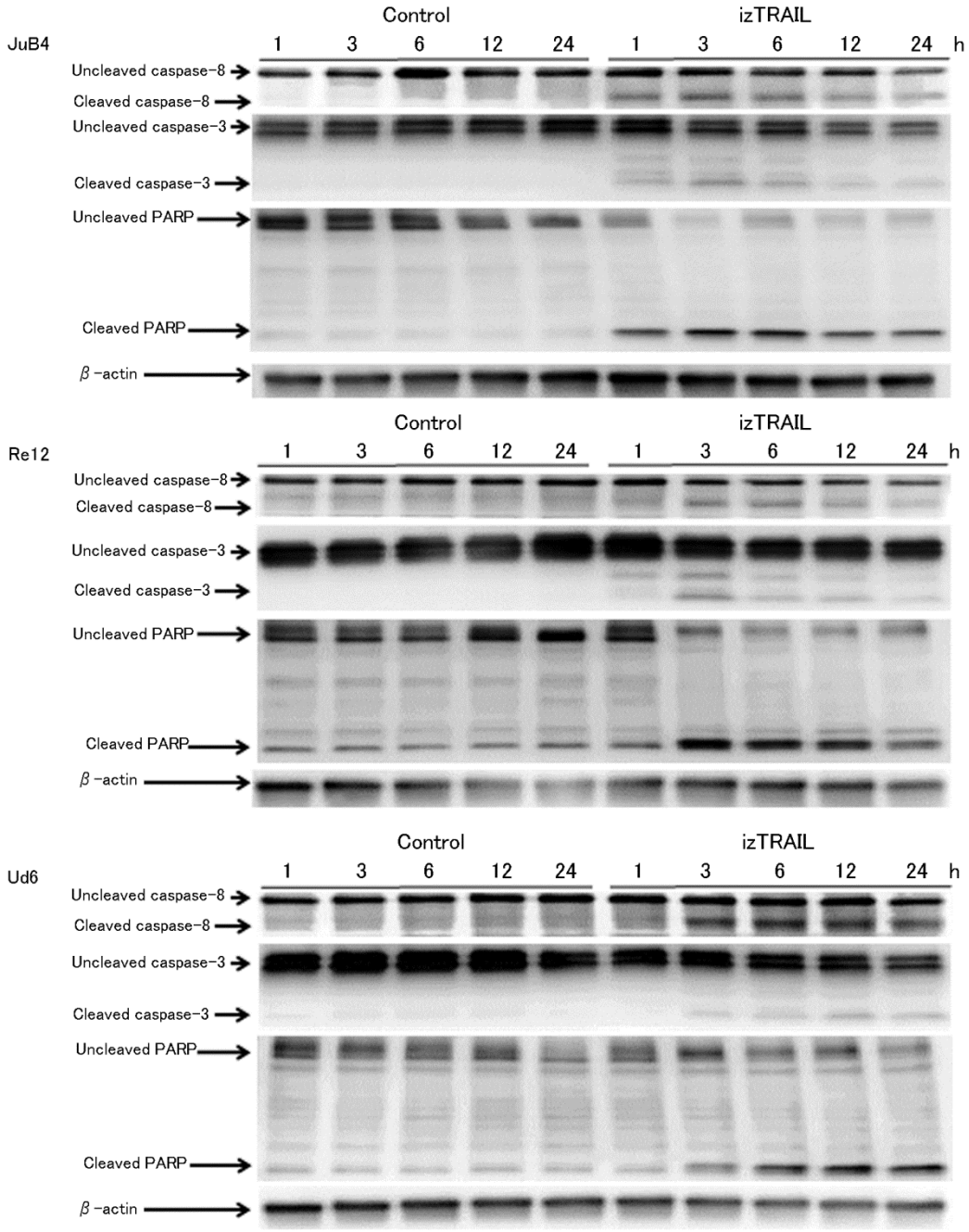

Fig. 1-6. Expression of caspase-8, caspase-3, and PARP.

Representative western blot bands are shown.

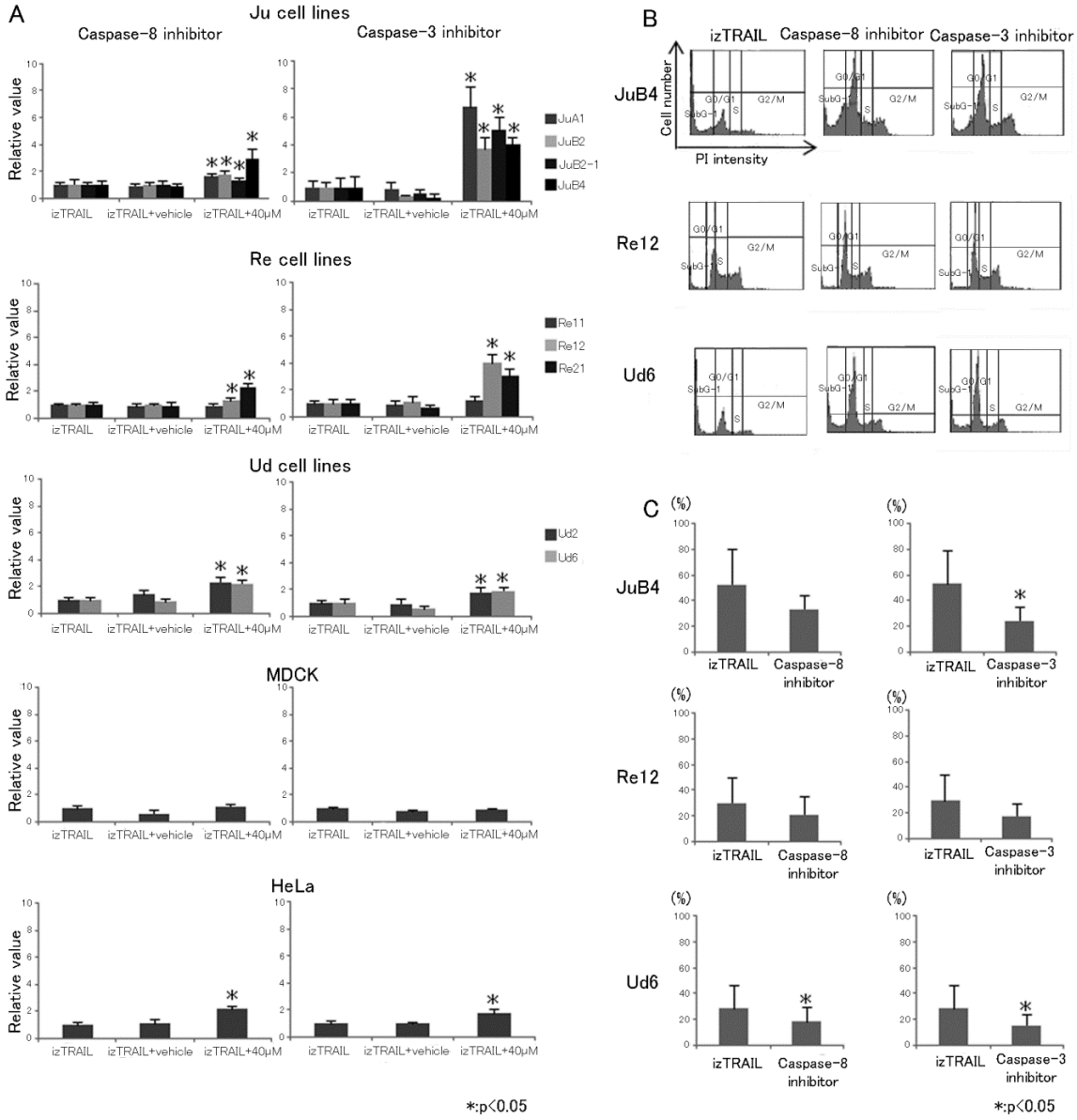

Fig. 1-7. izTRAIL-induced apoptosis is inhibited by treatment with caspase inhibitors.

A: Viability of canine HSA cell lines after incubation with caspase-8 or caspase-3 inhibitor and izTRAIL. The vertical axis shows the relative absorbance value compared with the control group and the horizontal axis shows different treatments: izTRAIL, izTRAIL and vehicle, and izTRAIL and 40 μM of caspase inhibitor. Representative results of more than three independent experiments are presented as the mean ± SD (*P < 0.05). B and C: JuB4, Re12, and Ud6 cells were treated with caspase inhibitors for 48 h and stained with PI. The vertical axis shows cell number and the horizontal axis shows PI staining intensity. The graphs show the percentages of cells in sub-G1 phase (*P < 0.05).

Chapter 2

The cytotoxic effect of izTRAIL to canine cell lines derived from mammary epithelial tumor

2.1 INTRODUCTION

CMT is the most common neoplasm in female dogs [83]. Histopathological examination is the gold standard diagnostic method for CMT, and in 2011, a new classification for CMT was proposed [42]. Based on this classification, the survival time for most aggressive tumor subtypes is approximately 3 months [108]. In addition, several studies have indicated that lymphatic vessel infiltration and regional lymph node metastasis of tumor cells are important to determine tumor prognosis, and the new classification of CMT is useful to predict the metastatic potential [107, 128, 132]. IMC, a malignant tumor subtype with invasion of dermal lymphatic vessels by neoplastic cells and inflammatory clinical signs, is the most aggressive CMT, with a poor prognosis [42, 76, 98]. Notably, IMC is a poor surgical candidate owing to its poor prognosis [121]. Furthermore, the combination of surgical resection and chemotherapy was used to treat mammary carcinomas but was ineffective against highly malignant tumors exhibiting lymphatic vessel infiltration [132]. Globally, human breast cancer (HBC) is the major cause of cancer death in women, with various therapeutic strategies available to treat HBC [41]. HBC and CMT have similar risk factors, clinical features, and molecular players such as hormones; therefore, CMT is considered a model for HBC [1, 100, 106]. Several studies investigating the TRAIL pathway in HBC and other tumors have designed various TRAIL

receptor-specific antibodies and some antibodies are undergoing clinical trials [15, 20, 54, 89, 105, 131, 133]. Furthermore, to enhance the sensitivity of the TRAIL-resistant tumors, several combinations with other molecules, such as MS-275 and caudatin, have also been studied in HBC [34, 119, 125, 134].

However, these studies have been mainly conducted in the medical field. In chapter 1, izTRAIL, which stably forms a trimer, was more effective in inducing apoptosis than the TRAIL monomer. This was the first study to report that the TRAIL trimer is more effective in dogs; this was similar to humans reports [138]. Although a study has reported the cytotoxic effect of TRAIL in canine epithelial tumors [123], the cytotoxic effect of izTRAIL has not been reported. In veterinary medicine, studies on such basic features of TRAIL are few, and no advances have been seen in the identification of receptors. Therefore, it is necessary to evaluate the TRAIL sensitivity, presence of TRAIL receptors, and TRAIL pathways in dogs, which will further aid in targeting the TRAIL receptors that chemotherapeutic agents target/bind to in humans. As a first step, it is important to confirm the conservation of TRAIL sensitivity in dog tumors. In this study, the cytotoxic effect of izTRAIL on CMT was investigated to accumulate basic information on the effect in various tumors. This study will provide the basis for future studies on TRAIL receptors and the TRAIL pathway in dogs.

2.2 MATERIALS AND METHODS

Case information

The three CMTs were collected from the Veterinary Teaching Hospital of Gifu University (VTH-GU), Gifu city, Japan. The characteristics of dogs with tumors are listed in Table 2-1. In the case of B101592, the dog had been treated at a private animal hospital for a mass in the mammary gland. Half a month later, an excision was performed at VTH-GU. In case of the Cha cells, the right mammary gland was swollen 10 days after the excision of the left mammary tumor at a private animal hospital. At the VTH-GU, a punch biopsy was performed 15 days after swelling developed. Lung metastasis was suspected following a computerized tomography scan. The dog died 38 days after the biopsy. In case of C090115, the dog had been treated for mastitis due to swollen mammary glands. However, no improvement was observed; hence, the dog was referred to the VTH-GU for a detailed examination 20 days later, and fine needle biopsy was performed with a 23 gauge-needle. Unfortunately, the prognosis details of B101592 and C090115 cases were lost. The two tumors (B101592 and Cha) obtained by biopsy were fixed with 10% buffered neutral formalin, embedded in paraffin, sectioned, and stained with hematoxylin and eosin (HE). These tumors were histologically classified into subtypes based on the 2011 classification [42]. Only cytological diagnosis was performed for C090115 using a Romanowsky-based stain (Hemacolor; Merck KGaA, Darmstadt, Germany) and no histopathological examination was performed at the owner's request.

Immunohistochemistry of original tumors

For immunohistochemical staining, B101592 and Cha sections were heated for 15 min at 121°C in a target retrieval solution (pH 6.0, Dako, Glostrup, Denmark). Next, the sections were incubated overnight at 4°C with the following primary antibodies: mouse anti-human cytokeratin (CK) monoclonal antibody (clone AE1/AE3, 1:10, Dako), mouse anti-vimentin monoclonal antibody (clone V9, 1:20, Dako), and murine anti-CK monoclonal antibody (clone CAM5.2, pre-diluted, BD Biosciences). The positive signal was visualized using 3, 3'-diaminobenzidine solution (Histofine SAB-PO (M) kit, Nichirei, Tokyo, Japan). Finally, the sections were counterstained with hematoxylin.

Cell culture

The B101592 and Cha tumor tissues were minced and sequentially digested with 0.1% collagenase Type I (Gibco, Carlsbad, CA, USA) at 37°C for 15 min and 0.25% trypsin-EDTA (Gibco) at 37°C for 15 min. Subsequently, the cell suspension was filtered through a 70-μm cell strainer (BD Biosciences) and resuspended in 10% FBS/D-MEM. In C090115, after cytological examination, the cells that remained in the needle and syringe were directly seeded in 10% FBS/D-MEM. All cells were cultured in a humidified incubator at 100% humidity, 37°C, 20% O_2, and 5% CO_2. Subconfluent cells were passaged after digestion with T/E solution. The cells were cultured with more than 60 passages.

To measure the growth curve and doubling time, all cells were plated in 24-well plates (ThermoFisher Scientific) at a cell density of 5000 cells/well in 1 m*l* of 10% FBS/D-MEM. The cells were collected using T/E solution and counted

once every 12 h using trypan blue in a Countess™ Automated Cell Counter (ThermoFisher Scientific). Triplicate wells were used for counting each cell.

Immunocytochemistry of cell lines

Prior to immunofluorescence analysis, the cells were cultured at a cell density of 2.0×10^4 cells/well in a chamber slide for 12 h. The cells were fixed with 100% methanol and incubated overnight at 4°C with the following primary antibodies: mouse anti-human CK monoclonal antibody (clone AE1/AE3, 1:20, Dako), mouse anti-vimentin monoclonal antibody (clone V9, 1:40, Dako), and murine anti-CK monoclonal antibody (clone CAM5.2, 1:10, BD Biosciences). Next, the cells were probed with anti-mouse IgG Fab2 Alexa Fluor® 488 (1:500, Cell Signaling Technology) secondary antibody. The slides were mounted with ProLong™ Diamond antifade Mountant with DAPI nuclear stain. The cells were analyzed under a fluorescence microscope.

Cell viability assay

Cell viability assays were performed using the premix WST-1 cell proliferation assay system as mentioned in chapter 1. The three cell lines, TRAIL/izTRAIL-resistant MDCK cells, and TRAIL/izTRAIL-sensitive HeLa cells were used in this study [31, 101]. MDCK cells were used as a negative control, while HeLa cells were used as a positive control. The cultured cells and HeLa cells were seeded in 96-well plates at a density of 1.0×10^4 cells/well. The MDCK cells were seeded at a density of 2.5×10^3 cells/well as they have a fast doubling time. The cells were cultured for 12 h. Next, the cells were cultured in 10%

FBS/D-MEM containing 0, 0.01, 0.1, 1.0, 10, or 100 ng/m*l* of izTRAIL for 24, 48, and 72 h. Subsequently, the cells were incubated with 10 μ*l* of WST-1 reagent for 1 h. Cell viability was quantified as the relative absorbance values of treated wells compared to those of the control (0 ng/m*l* izTRAIL) wells using the iMark™ microplate reader. The half-maximal inhibitory concentration (IC_{50}) of izTRAIL was calculated using Image J 1.51K based on the results of the viability assay.

Flow cytometric analysis of apoptosis

To detect changes in the cytoplasmic membrane that indicate early apoptosis, the cultured cells were treated with 100 ng/m izTRAIL for 18 h. The cells were collected using T/E solution, washed with D-PBS, and stained with the Alexa Fluor 488 Annexin V/Dead cell Apoptosis Kit.

To perform the cell cycle analysis, cell lines were treated with 100 ng/m*l* izTRAIL for 48 h. The supernatant and cells were collected using T/E solution and washed with D-PBS. Next, the collected cells were incubated with PI/RNase staining solution. The cells were counted using BD FACSCanto™ Ⅱ and analyzed using BD FACSDiva 6.1 software.

Analysis of nuclear fragmentation

The effect of izTRAIL on nuclear fragmentation was analyzed using fluorescence microscopy. The cultured cells were plated in 24-well plates at a density of 2.0×10^4 cells/well in 1 m*l* of 10% FBS/D-MEM for 12 h. The cells were treated with 100 ng/m*l* izTRAIL for 48 h and the cells were collected using T/E solution. The cells were washed with D-PBS and fixed in 4% paraformaldehyde

for 30 min. Next, the cells were placed on the slide and mounted with ProLong™ Diamond antifade Mountant containing DAPI nuclear stain. The DNA fragmentation was observed under a fluorescence microscope.

Western blotting

The effect of izTRAIL treatment on apoptosis-related proteins was evaluated by western blotting. Three cell lines were collected using a cell scraper at 1, 3, 6, 12, and 24 h after treatment with 100 ng/m*l* izTRAIL. The cells were then lysed with RIPA buffer containing proteinase inhibitor cocktail and EDTA. The concentration of the extracted protein was measured using the DC Protein assay kit. The protein concentration was determined from a standard curve of bovine serum albumin.

The protein samples were incubated with 4× Laemmli buffer and supplemented with 5% ß-mercaptoethanol at 95°C for 5 min. The proteins (15μg/lane) were resolved by SDS-PAGE and the resolved proteins were electroblotted onto a PVDF membrane at 60 V for 1.5 h at RT.

The PVDF membrane was incubated with 5% blocking reagent for 1 h at RT. Next, the PVDF membrane was probed with the following primary antibodies: mouse anti-human caspase-8 (1:2000, BD Biosciences), rabbit polyclonal anti-caspase-3 (1:1000, Cell Signaling Technology), mouse anti-PARP (1:2000, BD Biosciences), or ß-actin (1:1000, Cell Signaling Technology) for 1 h at RT. The primary antibodies were used after confirming that they had reacted with the proteins of the same size as reported in the previous study and chapter 1 for both HeLa and canine HSA cells, as established in the Department of

Veterinary Pathology, Gifu University [85].

The membrane was washed with TBS-T and incubated with the appropriate HRP-conjugated secondary antibody (anti-rabbit, 1:5000, Cell Signaling Technology or anti-mouse, 1:5000, Cell Signaling Technology) for 1 h at RT. The proteins were developed using Lumina Forte Western HRP Substrate and visualized using C-DiGit Blot scanner, and Image Studio Digits ver 4.0.

Inhibition of caspase-8 or caspase-3

The cell lines were cultured in 96-well plates for 12 h. Next, the cells were treated with 0, 2.5, 10, and 40 μM of caspase-8 inhibitor (Z-IETD-FMK) or caspase-3 inhibitor (Z-DEVD-FMK) for 2 h. The caspase inhibitors were dissolved in DMSO. Subsequently, the cells were treated with izTRAIL (at a final concentration 100 ng/m*l)* for 24 and 48 h. The WST-1 assay was performed as described in the cell viability assay.

To analyze the cell cycle, the cell lines were treated with caspase-8 and caspase-3 inhibitors before the addition of izTRAIL. Next, the tumor cells were collected and stained with PI/RNase staining solution. The cell cycle analysis was performed by flow cytometry as described previously.

Statistical analysis

All cell experiments were performed in triplicate at least. Cell viability assay results were statistically evaluated by one-way analysis of variance and Dunnet's posthoc test. The percentage of AnnexinV+/PI- cells or sub-G1 phase cells was compared between groups using the Student's t-test. These tests were

performed using BellCurve for Excel. All values are expressed as mean ± SD. The difference was considered statistically significant when the $P < 0.05$.

2.3 RESULTS

Tumor diagnosis and characteristics of cultured cells

The B101592 tumor tissue had papillary and ductal growth patterns, with a single layer of epithelial cells supported by fibrovascular stroma (Fig. 2-1A). Below the epithelial cells, a layer of myoepithelial cells was identified. These epithelial cells had an oval-shaped nucleus and eosinophilic cytoplasm. The nuclear and cellular pleomorphisms in the epithelial cells were not severe, and mitoses were rare. The epithelial cells were positive for CK AE1/AE3 and CK CAM5.2 (Fig. 2-1B and C). The myoepithelial cells were positive for vimentin, whereas the epithelial cells forming the duct were negative for vimentin (Fig. 2-1D).

The Cha tumor presented a solid growth pattern comprising of tightly packed cells (Fig. 2-1E). These cells had a round- to oval-shaped nucleus with prominent nucleoli and lightly basophilic to eosinophilic cytoplasm. Additionally, anisokaryosis was moderate, and mitoses were frequent in the Cha tumor cells. The tumor cells were partially positive for CK AE1/AE3 and CK CAM5.2, and positive for vimentin (Fig.2-1F, G and H). Based on the criteria proposed by Goldschmidt in 2011 [42], the B101592 tumor was classified as an intraductal papillary adenoma, while the Cha tumor was classified as carcinoma-solid.

The C090115 tumor had epithelial cells arranged in small clusters in cytological specimens (Fig. 2-1I), with round- to oval-shaped nucleus and scant to moderate amounts of deeply basophilic cytoplasm. The nucleus-to-cytoplasmic ratio of these cells was high. The nucleoli were large, prominent, and multiple. Based on the cytological diagnostic criteria [68], the C090115 tumor was

diagnosed as a malignant epithelial tumor, suspected as originating from the mammary gland.

The doubling times of the cultured cells derived from the B101592, Cha, and C090115 tumors were 19.1, 21.5, and 21.3 h, respectively (Fig. 2-2). The B101592 cultured cells had an oval-shaped nucleus and spindle to polygonal cytoplasm (Fig. 2-3A). Although some cells loosely adhered to each other and many cells were growing independently. Cha cultured cells had a round-shaped nucleus, abundant polygonal cytoplasm (Fig. 2-3B). These cells adhered to each other. C090115 cultured cells had a round- to oval-shaped nucleus and spindle to polygonal cytoplasm that adhered very tightly (Fig. 2-3C). C090115 cells had very prominent nucleoli. The cultured cells of B101592 and C090115 were positive for CK AE1/AE3 and CK CAM5.2, whereas those of Cha were negative (Fig. 3D, E, F, G, H, and I). All cultured cells were positive for vimentin (Fig. 3J, K, and L).

Cell viability and IC_{50} values

Treatment with izTRAIL decreased the cell viability in the three cultured cell lines, and HeLa cells depending on the concentration and treatment time. However, no significant cytotoxic effect of izTRAIL on MDCK cells was observed (Fig. 2-4). The IC_{50} values of izTRAIL in B101592, C090115, and Cha cells were 11.6±4.4, 5.45±2.2, and 14.9±6.9 ng/m*l*, respectively at 72 h post-treatment. The IC_{50} value of izTRAIL in HeLa cells was 13.76±0.9 ng/m*l* at 72 h post-treatment, which was similar to the IC_{50} value reported in chapter 1.

Morphological changes in cultured cells and analysis of apoptosis

Morphologically, the cultured cells were small and round and were detached from the dishes after treatment with izTRAIL for 18 h (Fig. 2-5). Flow cytometric analysis revealed that the proportion of early apoptosis phase cells (AnnexinV+/PI- cells) increased 18 h post-izTRAIL treatment.

DAPI staining revealed nuclear fragmentation in the cultured cells at 48 h post-izTRAIL treatment. Additionally, the cell cycle analysis revealed that the proportion of cells in the sub-G1 phase markedly increased, whereas the proportion of cells in the G0/G1 phase decreased after treatment with izTRAIL (Fig. 2-6).

The expression of caspase-8, caspase-3, and PARP after izTRAIL treatment was detected in the three cell lines using western blotting (Fig. 2-7). The expression levels of cleaved caspase-8, cleaved caspase-3, and cleaved PARP increased, whereas the expression of non-cleaved caspase-8, non-cleaved caspase-3, and non-cleaved PARP decreased in the B101592 cells after izTRAIL treatment for 1 h compared to the controls. Non-cleaved PARP was not detectable between 3 and 24 h. The expression levels of cleaved caspase-8 and cleaved PARP increased after izTRAIL treatment for 3 h, whereas those of cleaved caspase-3 were detectable after izTRAIL treatment for 6 h in the C090115 and Cha cells. In C090115 cells, non-cleaved PARP was not detectable after 24 h. Furthermore, non-cleaved PARP was not detectable after 12-24 h in the Cha cells.

The WST-1 assay after treatment with the caspase inhibitor revealed that both caspase-3 and caspase-8 inhibitors significantly increased the tumor cell viability at 40 μM (Fig. 2-8). The flow cytometric analysis demonstrated that

caspase-8 and caspase-3 inhibitors decreased the proportion of cells in the sub-G1 phase and increased the proportion of cells in the G0/G1 phase (Fig. 2-9).

2.4 DISCUSSION

In this study, the cytotoxic effects of izTRAIL against cultured cells derived from the mammary gland tissue tumors, including histologically low-grade tumor (B101592), histologically malignant tumor (Cha), and cytologically malignant epithelial tumor (C090115), were evaluated. The clinical course and histopathology suggested that Cha may be an inflammatory breast cancer, but no obvious tumor embolization into the dermal lymphatic vessels was observed in the sampled tissues. C090115 demonstrated a high degree of malignancy of the epithelial component and clinical signs of inflammation; hence, the possibility of inflammatory breast cancer cannot be denied. All three cultured cell lines were positive for vimentin. B101592 and C090115 cells were positive for CK AE1/AE3 and CK CAM5.2, suggesting that B101592 and C090115 tumors were derived from the epithelial cells in the mammary gland (except squamous epithelial cells) as CMT cell lines are reported to be positive for vimentin in several cases [50, 51, 147]. Cha cells were negative for both CK AE1/AE3 and CK CAM5.2. However, Cha cells adhered to each other, indicating that they were epithelial cells. In the biopsied specimens, Cha cells were partially positive for CK AE1/AE3 and CK CAM5.2, while they were homogenously positive for vimentin. This indicated that the cultured cells were derived from the CK AE1/AE3 and CK CAM5.2 negative area of the tumor. There are some established CMT cell lines that are positive for vimentin and weakly positive or negative for cytokeratin depending on their passage number [50, 147]. The results of this study and those from previous reports suggested that the three cultured cell lines were derived from CMT cells. However, to prove that these cell

lines are CMT cells, it is necessary to transplant these cultured cells into mice, evaluate their tumorigenicity, tissue morphology, metastatic ability, and confirm their tumor reproducibility. In the future, xenograft models with these cell lines must be created to establish them as new CMT cell lines.

In this study, izTRAIL induced apoptosis as well as the activation of caspase-8 and caspase-3 in cultured cells derived from CMT, which was also observed in the canine HSA cells. TRAIL activates caspase-8, which activates both extrinsic and intrinsic pathways in p53-independent or dependent manner [22, 89]. In the first chapter, it is suggested that TRAIL is effective against canine tumors with p53 inactivation. In this chapter, we did not evaluate the presence of p53 abnormality in cultured cell lines, as mutations in *p53* are reported in spontaneous CMT and cell lines [1, 21, 72, 88, 106]. Therefore, p53-independent anti-tumor drugs, such as TRAIL can be expected to be effective in CMT with p53 inactivation.

In addition, the IC_{50} values of izTRAIL against cultured cells derived from CMT were equivalent to those observed in the canine HSA cell lines. Spee *et al.* [123] reported that the IC_{50} value of the TRAIL monomer against CMT cell (P114) was approximately in the range of 5-15 ng/m*l*, consistent with previous studies which had reported that the sensitivity to TRAIL/izTRAIL largely differs depending on the cell lines [22, 123, 134, 138, 142]. The three cell lines demonstrated sufficient sensitivity to izTRAIL when compared to the HeLa and MDCK cells; the P114 cells are very sensitive to TRAIL [123]. The differential TRAIL sensitivity of the cell lines derived from breast cancer has been previously reported in humans [84]. Downregulation of XIAP, which directly binds and

inhibits caspase-3, 7 and 9, enhanced the sensitivity of tumors to TRAIL [89, 123, 134]. In this study, the expression of non-cleaved PARP was not detected at 24 h post-izTRAIL treatment in all cell lines, indicating that caspase-3 was sufficiently activated. This suggested that XIAP is unlikely to be involved in inhibiting apoptosis in the three evaluated cell lines. Additionally, the overexpression of survivin, which belongs to the same family as XIAP, was reported in the canine spontaneous mammary tumors [12]. In human medicine, various molecules that suppress the anti-apoptotic factors such as XIAP and survivin also enhance the sensitivity to TRAIL [134]. Therefore, this suggested that these molecules may increase the sensitivity of canine tumors to TRAIL.

In the first chapter, it is described that there are very limited knowledge available on the canine TRAIL receptor. Treatment with izTRAIL induced apoptosis in canine HSA and cultured cells derived from CMT. This indicated that canine tumor cells express a certain level of the conservative TRAIL receptor, which has a death domain capable of activating caspase-8. Western blot analysis revealed that the B101592 cells exhibited the earliest response to izTRAIL. As caspase-8 activation is the first step in the TRAIL pathway, the difference in reactivity may involve competitive factors upstream of caspase-8. One possible explanation is that the expression level of TRAIL receptors differs among the tumor cells. Further studies on the TRAIL receptor are crucial to confirm this hypothesis. Another possible explanation is that the function of caspase-8 is inhibited by c-FLIP, which has sequence homology with caspase-8 and competes with caspase-8 to bind FADD [89, 134]. FVP enhances the TRAIL sensitivity of the TRAIL-resistant HBC cell lines by downregulating the

expression of c-FLIP, and this molecule is reported to exhibit similar effects in canine lymphoma cell lines [93, 97]. Further investigations evaluating the effect of c-FLIP in CMT cells after the administration of FVP need to be performed.

2.5 SUMMARY

The three cell lines were cultured from three CMTs. These cell lines have the characteristics of epithelial cells. In this study, izTRAIL indicated adequate cytotoxicity in these canine cell lines, as well as canine HSA cell lines. The cytotoxicity of izTRAIL was attributed to apoptosis, owing to cell membrane alterations, nuclear fragmentation, caspase-8 and -3 activation, and PARP cleavage. This study suggests that apoptosis induced by TRAIL is associated with the DR, which is widely conserved in canine tumor cells. The results in the present study support the versatility of TRAIL and provide the basis for future studies on the TRAIL receptor and TRAIL pathway in dogs.

TABLE AND FIGURES

Table 2-1 An information of original tumors

	Breed	Age	Sex
B101592	Toy poodle	9y7m	F
Cha	Beagle	13y2m	F
C090115	Labrador retriever	10y9m	SF

F; Female, SF; Spayed Female

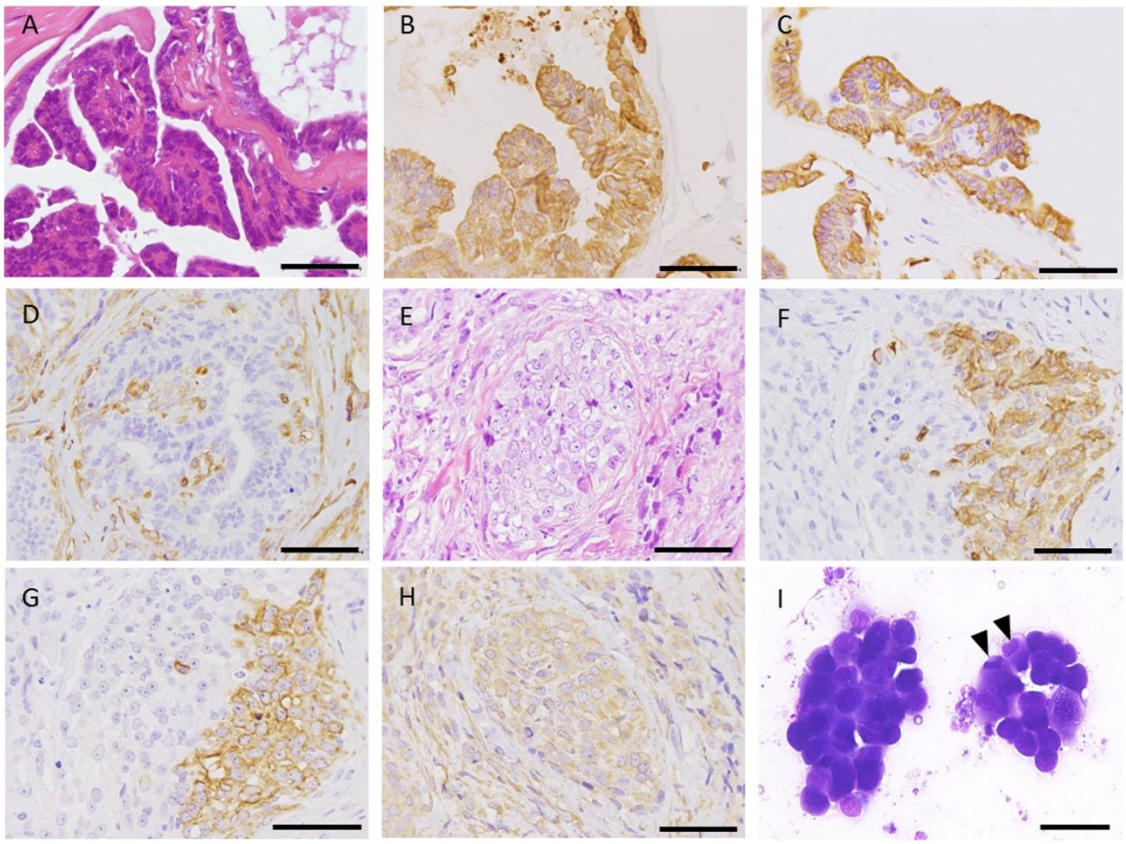

Fig.2-1. Biopsy and fine-needle aspiration of original tumors

The papillae are covered with a single layer of epithelial cells in the B101592 tumor. HE staining (A). Tumor cells are positive for cytokeratin (CK) AE1/AE3 (B) and CK CAM5.2 (C), and negative for vimentin (D). Tumor cells are packed tightly without tubular differentiation in the Cha tumors. HE staining (E). The tumor cells are partially positive for CK AE1/AE3 (F), CK CAM5.2 (G), and positive for vimentin (H). The epithelial cells show round to oval-shaped nucleus and scant to moderate amount of deeply basophilic cytoplasm in C090115 (I). Arrowheads show mitoses. Hemacolor stain. Bar=50 μm.

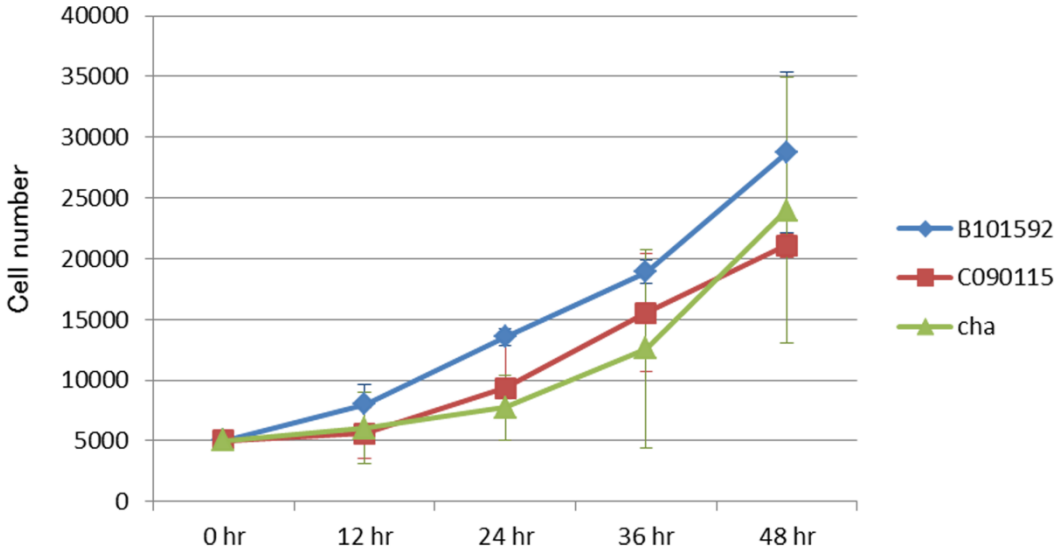

Fig. 2-2. Growth rate of cultured cells derived from the canine mammary gland

The vertical axis represents the cell number, and the horizontal axis represents the time. The graph is presented as mean ± SD.

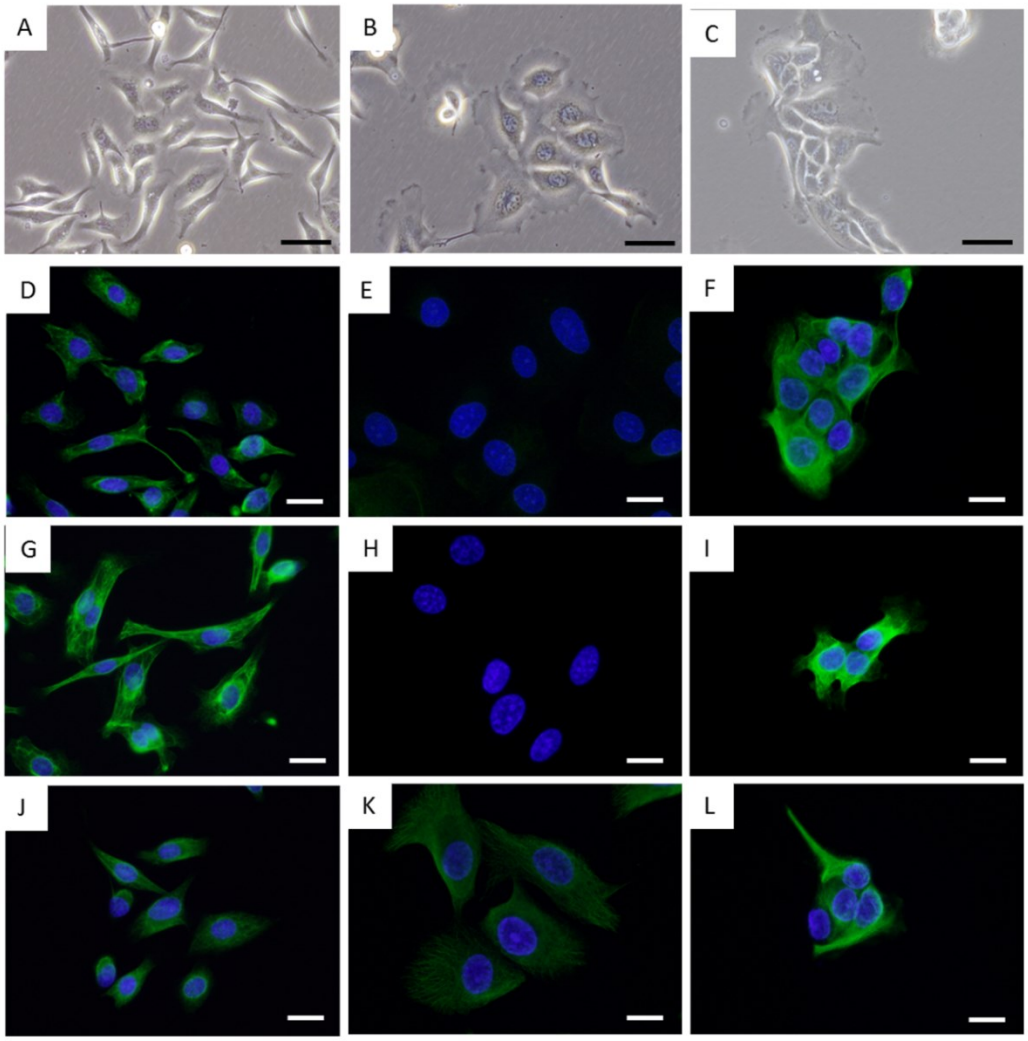

Fig.2-3. Morphological and immunocytological characteristics of cultured cells

Cultured cells derived from B101592 tumor show round-to oval-shaped nucleus and spindle to polygonal cytoplasm (A). Cultured cells derived from Cha tumor show oval-shaped nucleus and abundant polygonal cytoplasm (B). Cultured cells derived from C090115 tumor show round- to oval-shaped nucleus and polygonal cytoplasm adhered to each other very tightly (C). Bar=50 μm. In immunofluorescence analysis, B101592 cells are positive for CK AE1/AE3 (D), CK CAM5.2 (G), and vimentin (J). Cha cells are positive for vimentin (K), but negative for CK AE1/AE3 (E) and CK CAM 5.2 (H). C090115 cells are positive for CK AE1/AE3 (F), CK CAM5.2 (I), and vimentin (L). Bar=20 μm

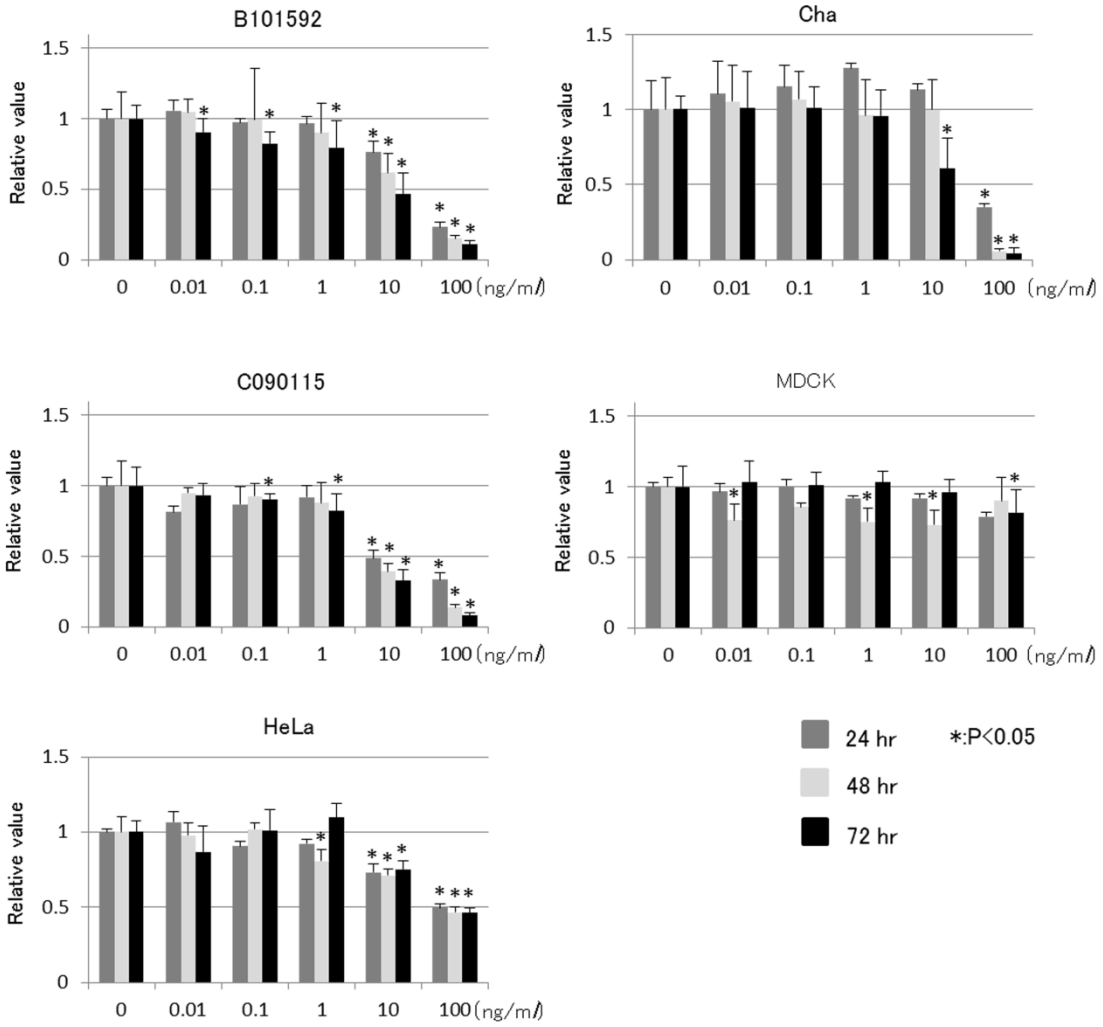

Fig.2-4. Cell viability of cultured cells, MDCK cells, and HeLa cells after izTRAIL treatment

The vertical axis represents the relative absorbance value compared with the control group (no izTRAIL treatment), and the horizontal axis represents the concentration of izTRAIL. Representative results of more than three independent experiments are presented as mean ± SD (*$P < 0.05$).

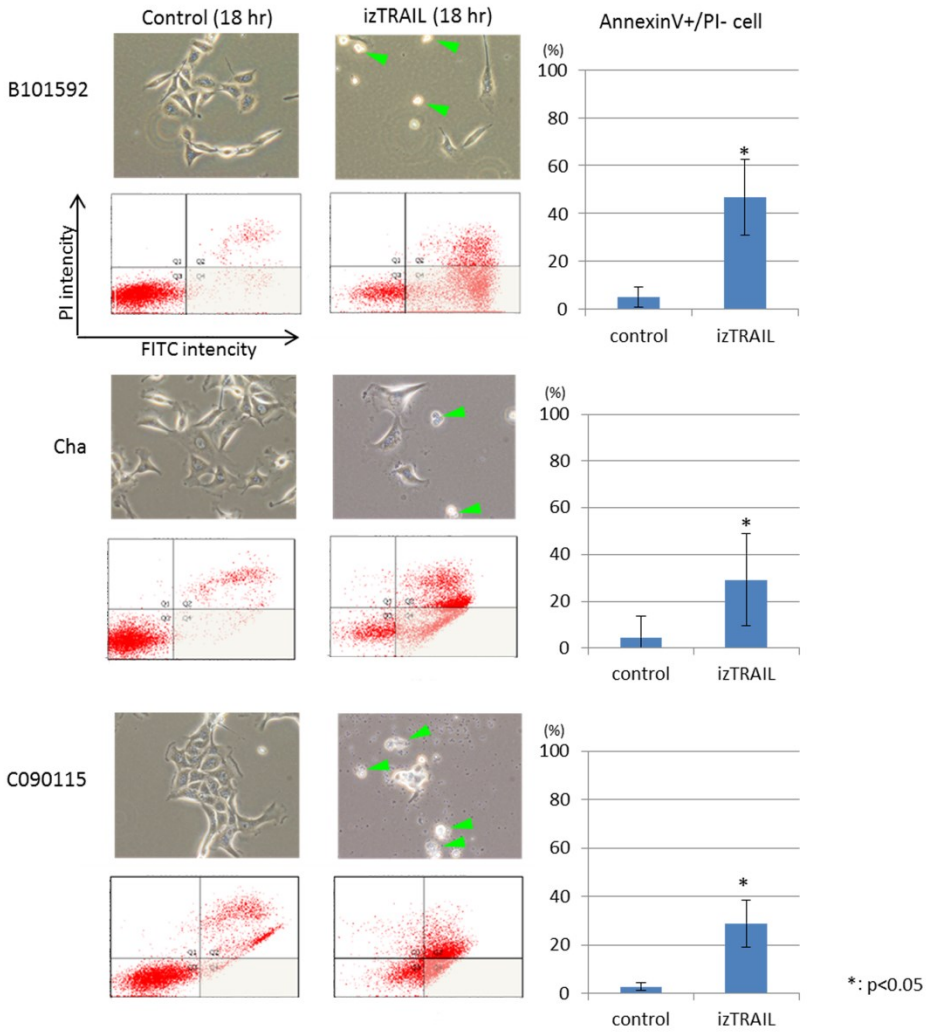

Fig.2-5. Cellular morphological changes and percentage of Annexin V+/ PI- cells after incubation with izTRAIL

The image shows cultured cells treated with 100 ng/m*l* of izTRAIL for 18 h; the cells were detached from dishes as small round (arrowheads) after izTRAIL treatment. The dot plots under the photo show the cells stained with Annexin V/PI. The vertical axis represents the PI staining intensity and the horizontal axis represents the Annexin V staining intensity. The cells in the gray area are Annexin V+/PI- (apoptotic cells). Graph on the right indicating mean percentage of Annexin V+/PI- cells from replicate experiments. The Annexin V+/PI- cells increased significantly after izTRAIL treatment (*P < 0.05).

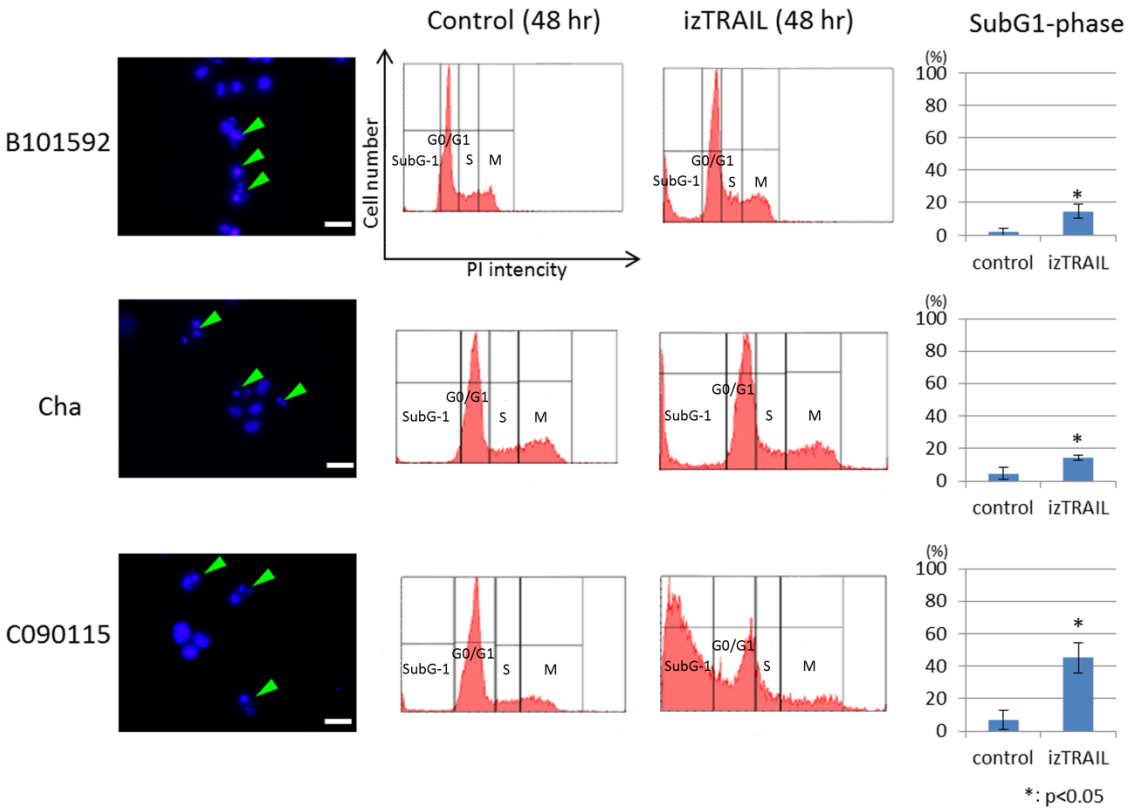

Fig.2-6. Nuclear fragmentation induced by izTRAIL

The images obtained from DAPI staining show the nuclear morphology changes after treatment with 100 ng/m*l* of izTRAIL for 48 h. Arrowheads show the nuclear fragments. Representative DNA histogram at right showing the cells stained with PI for each cell. The vertical axis represents the cell number, and the horizontal axis represents the PI staining intensity. The percentage of cells in the sub-G1 phase is shown in the graph. The proportion of cells in the sub-G1 phase increased significantly after treatment with izTRAIL (*P < 0.05).

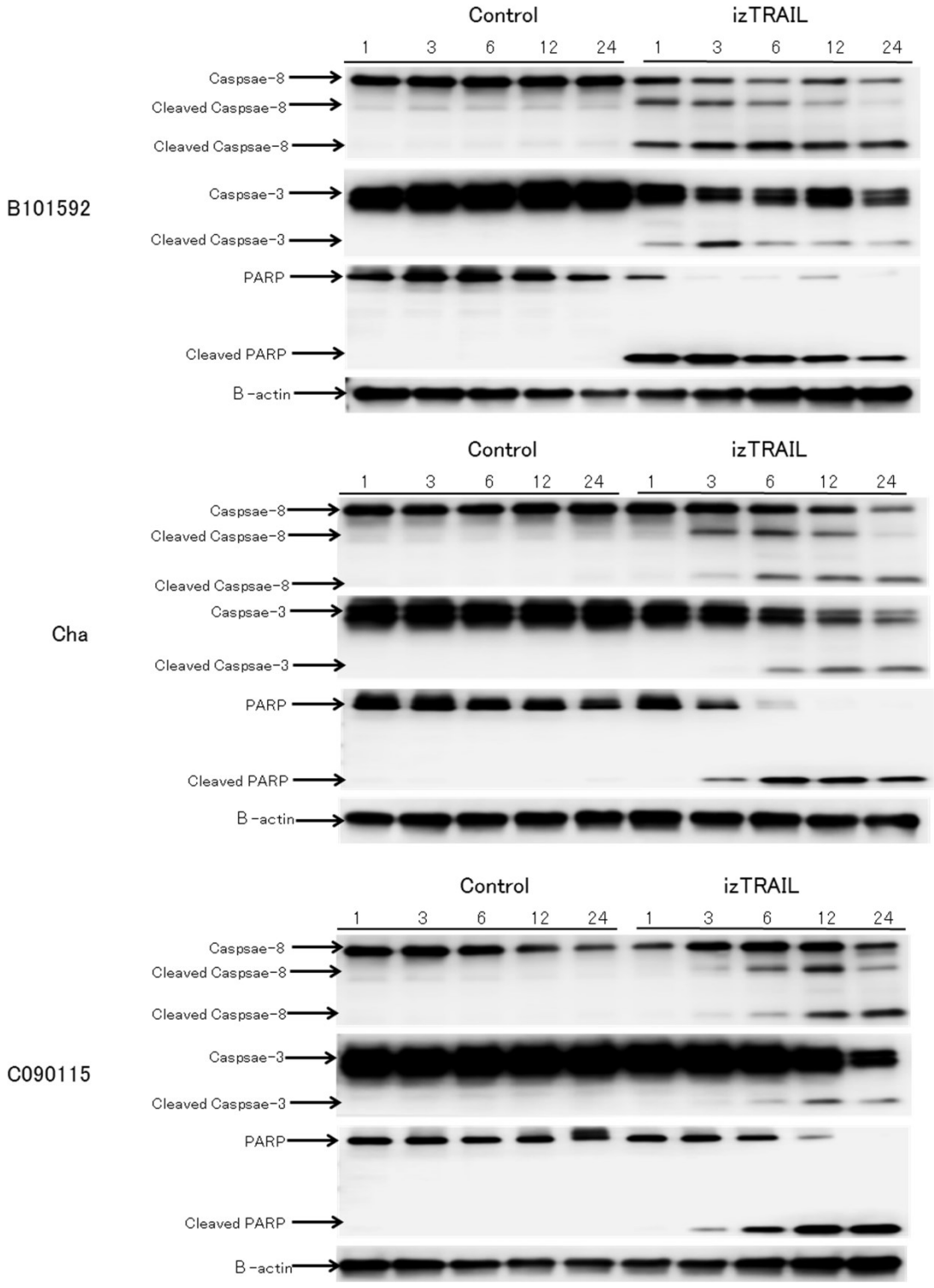

Fig.2-7. Expression of caspase-8, caspase-3, and PARP

Representative western blot bands are shown.

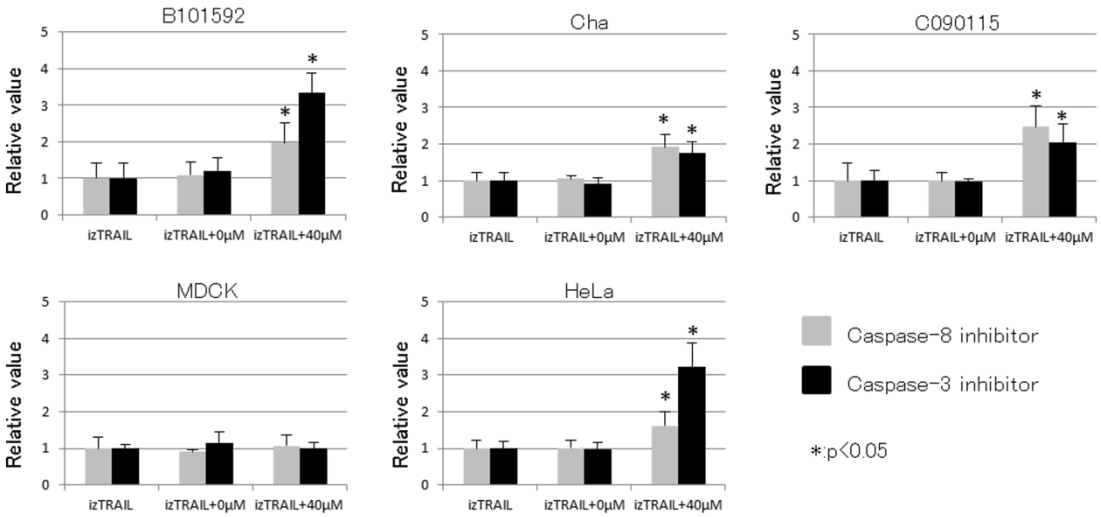

Fig.2-8. Viability of cultured cells after treatment with caspase inhibitor and izTRAIL

Viability of cultured cells after treatment with caspase-8 or caspase-3 inhibitor and izTRAIL. The vertical axis represents the relative absorbance value compared with the control group, and the horizontal axis represents different treatments: izTRAIL, izTRAIL and vehicle, and izTRAIL and 40 μM of caspase inhibitor. Representative results of more than three independent experiments are presented as mean ± SD (*P < 0.05).

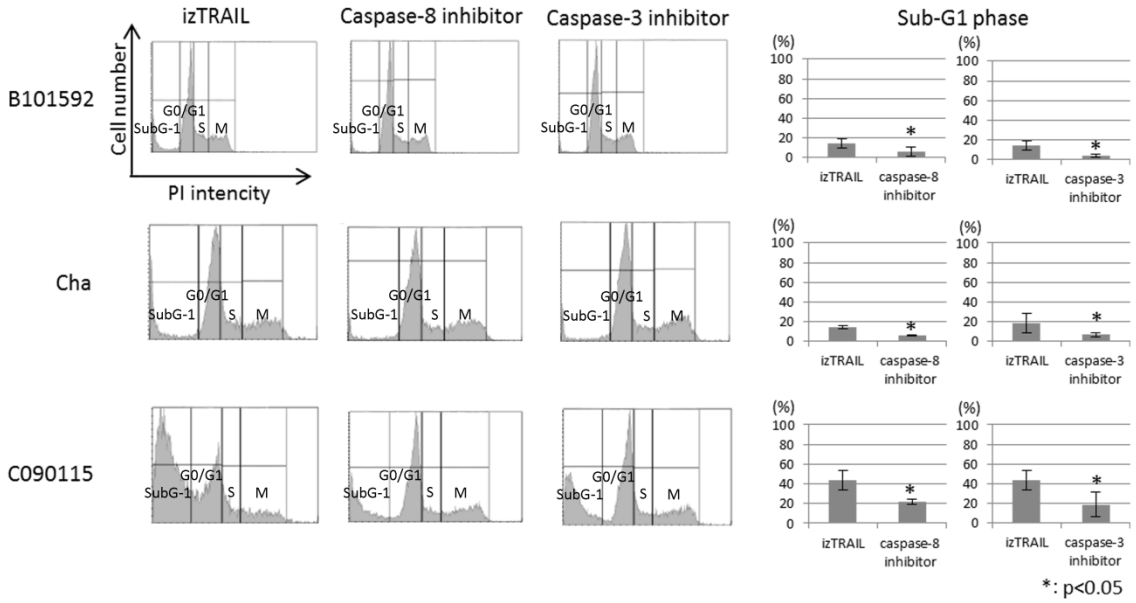

Fig.2-9. Effect of caspase inhibitors on the proportion of cells in sub-G1 phase

Three cell lines were treated with caspase inhibitors and izTRAIL for 48 h and stained with PI. The vertical axis represents cell number, while the horizontal axis represents PI staining intensity. The graphs show the percentages of cells in sub-G1 phase (*$P < 0.05$).

CONCLUSION

Some canine malignant tumors are similar to human tumors in terms of the risk factors, genetic mutations associated with tumorigenesis, and histological characteristics of the tumor. Thus, they serve as exceptional models for spontaneous human tumors. HSA, a rare tumor in humans, occurs frequently in dogs. As in humans, canine HSA is highly malignant with a very poor prognosis despite surgical intervention and chemotherapy during early metastasis and dissemination. Recently, the molecular characteristics of canine HSA have been elucidated. However, no effective treatment strategy has so far been developed. CMT, another tumor that can serve as a human model, is the most common tumor in female dogs, and 20-80% are malignant. High-grade CMT with vascular invasion is difficult to treat and has a poor prognosis. In addition to research as an animal model for human breast cancers, the development of new therapies for CMT is needed because of its veterinary clinical importance.

In clinical medicine, TRAIL is one of the most prominent anti-tumor cytokines. As TRAIL induces apoptosis selectively in tumor cells with no effect on normal cells, it can be used to treat various tumors without severe systemic side effects. Additionally, TRAIL activates both extrinsic and intrinsic pathways; it induces p53-independent or -dependent apoptosis. Several reports have demonstrated the effects of TRAIL in various tumors, along with the mechanism of tumor resistance. However, no study has evaluated its effects on HSA in the medical field. In the field of veterinary medicine, there are few reports evaluating the effects of TRAIL on tumor cells. Furthermore, the mechanism of action of TRAIL has rarely been studied. Therefore, we aimed to verify the effects

of TRAIL on HSA so as to accumulate fundamental information necessary for future TRAIL research in veterinary medicine.

In chapter 1, the cytotoxicity of TRAIL in canine HSA cell lines was evaluated. Of the three human recombinant TRAILs tested, izTRAIL, which formed a stable trimer, was most effective to reduce cell viability in canine HSA cell lines. On the contrary, izTRAIL did not affect the cell viability of normal canine vascular endothelial cells, indicating that the cytotoxic effect of izTRAIL was selective to tumor cells. izTRAIL increased the number of tumor cells in the early apoptotic phase, demonstrated by the presence of annexin V positive and PI negative cells. Nuclear fragmentation was observed by DAPI staining. There was an increase in the number of sub-G1 phase cells stained with PI after izTRAIL treatment. In addition, activation of caspase-8 and caspase-3, and degradation of PARP was also observed after izTRAIL treatment. These TRAIL effects were suppressed by the inhibition of caspase-8 and caspase-3. The aforementioned results indicate that izTRAIL induces caspase-8-mediated apoptosis in canine HSA cell lines.

In chapter 2, the effect of izTRAIL was evaluated in cell lines derived from CMT. Cells collected from one benign CMT and two malignant CMTs were cultured over 60 passages. The cultured cells had the characteristics of epithelial tumors as indicated by the cell morphology and immunofluorescence staining. Following izTRAIL treatment, the viability of these three cell lines was reduced. The number of cells in the early apoptotic phase demonstrating annexin V positive and PI negative was increased. Nuclear fragmentation was observed following DAPI staining. There was an increase in the number of sub-G1 phase cells stained with PI. Caspase-8 and caspase-3 were activated by izTRAIL

treatment, with PARP degradation also observed. These changes were suppressed by caspase-8 and caspase-3 inhibition. Based on these results, we concluded that izTRAIL is capable of inducing caspase-8-mediated apoptosis in cell lines derived from CMT, as well as canine HSA cell lines.

In this study, izTRAIL induced apoptosis via caspase-8 activation on canine cell lines derived from HSA and CMT, without any cytotoxic effect on normal cells. izTRAIL also induced apoptosis in HSA cells with p53 abnormalities. Thus, TRAIL may be useful for the treatment of HSA with p53 inactivation and in several tumors in veterinary medicine.

ACKNOWLEDGEMENTS

I deeply appreciate my chief supervisor, Associate Prof. Dr. Hiroki Sakai, for his accurate advice and instructions, polite suggestions, and criticisms. Furthermore, I am deeply indebted to my secondary supervisors, Prof. Dr. Yoshiyasu Kobayashi, Prof. Dr. Kenji Ochiai, Prof. Dr. Makoto Shibutani, Prof. Dr. Takashi Mori, and Prof. Tokuma Yanai for carefully reading my manuscript and providing polite suggestions. I would like to thank Assistant Prof. Dr. Akihiro Hirata, Assistant Prof. Dr. Mami Murakami, Dr. Kayoko Yonemaru, and members of the Veterinary Pathology laboratory for their kind support during this research.

REFERENCES

1. Abdelmegeed, S. M. and Mohammed, S. 2018. Canine mammary tumors as a model for human disease (Review). *Oncol. Lett.* **15**: 8195–8205.
2. Abou Asa, S., Mori, T., Maruo, K., Khater, A., El-sawak, A., Abd el-Aziz, E., Yanai, T. and Sakai, H. 2015. Analysis of genomic mutation and immunohistochemistry of platelet-derived growth factor receptors in canine vascular tumours. *Vet. Comp. Oncol.* **13**: 237–245.
3. Abou Asa, S., Murai, A., Murakami, M., Hoshino, Y., Mori, T., Maruo, K., Khater, A., El-sawak, A., Abdo el-Aziz, E., Yanai, T. and Sakai, H. 2012. Expression of platelet-derived gowth factor and its receptors in spontaneous canine hemangiosarcoma and cutaneous hemangioma. *Histol. Histopathol.* **27**: 601–607.
4. Adachi, M., Hoshino, Y., Izumi, Y., Sakai, H. and Takagi, S. 2016. Effects of inhibitors of vascular endothelial growth factor receptor 2 and downstream pathways of receptor tyrosine kinases involving phosphatidylinositol 3-kinase/Akt/mammalian target of rapamycin or mitogen-activated protein kinase in canine hemangiosar. *Can. J. Vet. Res.* **80**: 209–216.
5. Adams, V. J., Evans, K. M., Sampson, J. and Wood, J. L. N. 2010. Methods and mortality results of a health survey of purebred dogs in the UK. *J. Small Anim. Pract.* **51**: 512–524.
6. Alberts, B., Johnson, A., Lewis, J., Morgan, D., Raff, M., Roberts, K. and Walter, P. 2015. Cell death. pp. 1023–1024. *In*: *Molecular biology of the cell*, 6th ed., (Wilson, John and Hunt, Tim eds.) Garland Science, New York.
7. Allen, J. E., Crowder, R. and El-Deiry, W. S. 2015. First-in-class small

molecule ONC201 induces DR5 and cell death in tumor but not normal cells to provide a wide therapeutic index as an anti-cancer agent. *PLoS One*. **10**: 1–9.

8. Allen, J. E., Crowder, R. and El-Deiry, W. S. 2016. First-in-class small molecule ONC201 induces DR5 and cell death in tumor but not normal cells to provide a wide therapeutic index as an anti-cancer agent. *PLoS One*. **11**: 1–1.

9. Allen, J. E., Krigsfeld, G., Mayes, P. A., Patel, L., Dicker, D. T., Patel, A. S., Dolloff, N. G., Messaris, E., Scata, K. A., Zhou, J., Wu, G. S. and El-deiry, W. S. 2013. Dual inactivation of Akt and ERK by TIC10 signals Foxo3a nuclear translocation, TRAIL gene induction, and potent antitumor effects. *Sci Transl Med*. **5**: 1–23.

10. Ashkenazi, A., Pai, R. C., Fong, S., Leung, S., Lawrence, D. A., Marsters, S. A., Blackie, C., Chang, L., McMurtrey, A. E., Hebert, A., DeForge, L., Koumenis, I. L., Lewis, D., Harris, L., Bussiere, J., Koeppen, H., Shahrokh, Z. and Schwall, R. H. 1999. Safety and antitumor activity of recombinant soluble Apo2 ligand. *J. Clin. Invest.* **104**: 155–162.

11. Batschinski, K., Nobre, A., Vargas-Mendez, E., Tedardi, M. V., Cirillo, J., Cestari, G., Ubukata, R. and Dagli, M. L. Z. 2018. Canine visceral hemangiosarcoma treated with surgery alone or surgery and doxorubicin: 37 cases (2005-2014). *Can. Vet. J.* **59**: 967–972.

12. Bongiovanni, L., Romanucci, M., Malatesta, D., D'Andrea, A., Ciccarelli, A. and Della Salda, L. 2015. Survivin and related proteins in canine mammary tumors: Immunohistochemical expression. *Vet. Pathol.* **52**: 269–

275.

13. Brown NO, Patnaik AK, M. E. 1985. Canine hemangiosarcoma: Retrospective analysis of 104 cases. *J Am Vet Med Assoc*. **186**: 56–58.

14. Buchbinder, E. I., Dutcher, J. P., Daniels, G. A., Curti, B. D., Patel, S. P., Holtan, S. G., Miletello, G. P., Fishman, M. N., Gonzalez, R., Clark, J. I., Richart, J. M., Lao, C. D., Tykodi, S. S., Silk, A. W. and McDermott, D. F. 2019. Therapy with high-dose Interleukin-2 (HD IL-2) in metastatic melanoma and renal cell carcinoma following PD1 or PDL1 inhibition. *J. Immunother. Cancer*. **7**: 1–7.

15. Buchsbaum, D. J., Oliver, P. G., Hammond, C. J., Zhou, T., Zhang, S., Carpenter, M., LoBuglio, A. F. and Grizzle, W. E. 2003. Antitumor efficacy of TRA-8 anti-DR5 monoclonal antibody alone or in combination with chemotherapy and/or radiation therapy in a human breast cancer model. *Clin. Cancer Res.* **9**: 3731–3741.

16. Burton, J. H., Venable, R. O., Vail, D. M., Williams, L. E., Clifford, C. A., Axiak-Bechtel, S. M., Avery, A. C. and Thamm, D. H. 2015. Pulse-administered toceranib phosphate plus lomustine for treatment of unresectable mast cell tumors in dogs. *J. Vet. Intern. Med.* **29**: 1098–1104.

17. Caceres, S., Monsalve, B., Peña, L., de Andres, P. J., Alonso-Diez, A., Illera, M. J., Woodward, W. A., Reuben, J. M., Silvan, G. and Illera, J. C. 2018. In vitro and in vivo effect of flutamide on steroid hormone secretion in canine and human inflammatory breast cancer cell lines. *Vet. Comp. Oncol.* **16**: 148–158.

18. Carlson, A., Alderete, K. S., Grant, M. K. O., Seelig, D. M., Sharkey, L. C.

and Zordoky, B. N. M. 2017. Anticancer effects of resveratrol in canine hemangiosarcoma cell lines. *Vet. Comp. Oncol.* 1–9.

19. Carlsten, K. S., London, C. A., Haney, S., Burnett, R., Avery, A. C. and Thamm, D. H. 2012. Multicenter prospective trial of hypofractionated radiation treatment, toceranib, and prednisone for measurable canine mast cell tumors. *J. Vet. Intern. Med.* **26**: 1–16.

20. Cheng, A. L., Kang, Y. K., He, A. R., Lim, H. Y., Ryoo, B. Y., Hung, C. H., Sheen, I. S., Izumi, N., Austin, T., Wang, Q., Greenberg, J., Shiratori, S., Beckman, R. A. and Kudo, M. 2015. Safety and efficacy of tigatuzumab plus sorafenib as first-line therapy in subjects with advanced hepatocellular carcinoma: A phase 2 randomized study. *J. Hepatol.* **63**: 896–904.

21. Chu, L. L., Kong, J. M. C., Ghahremani, M., Schmeing, M., Pelletier, J., Rutteman, G. R., Misdorp, W. and Van Garderen, E. 1998. Genomic organization of the canine p53 gene and its mutational status in canine mammary neoplasia. *Breast Cancer Res. Treat.* **50**: 11–25.

22. Cretney, E., Takeda, K. and Smyth, M. J. 2007. Cancer: Novel therapeutic strategies that exploit the TNF-related apoptosis-inducing ligand (TRAIL)/TRAIL receptor pathway. *Int. J. Biochem. Cell Biol.* **39**: 280–286.

23. Danial, N. N. and Korsmeyer, S. J. 2004. Cell death: Critical control points. *Cell.* **116**: 205–219.

24. De, C. H., Toledo-Piza, E., Amorin, R., Barboza, A. and Tobias, K. M. 2009. Inflammatory mammary carcinoma in 12 dogs: Clinical features, cyclooxygenase-2 expression, and response to piroxicam treatment. *Can. Vet. J.* **50**: 506–510.

25. Degli-Esposti, M. a, Dougall, W. C., Smolak, P. J., Waugh, J. Y., Smith, C. a and Goodwin, R. G. 1997. The novel receptor TRAIL-R4 induces NF-kappaB and protects against TRAIL-mediated apoptosis, yet remains an incomplete death domain. *Immunity*. **7**: 813–820.

26. Degli-Esposti, M. A., Smolak, P. J., Walczak, H., Waugh, J., Huang, C.-P., DuBose, R. F., Goodwin, R. G. and Smith, C. A. 1997. Cloning and characterization of TRAIL-R3, a novel member of the emerging TRAIL receptor family. *J. Exp. Med.* **186**: 1165–1170.

27. Díaz-Vélez, J. C., Ahlers, M., Desiati, P. and Fiorino, D. 2017. A review of systematic reviews of the cost-effectiveness of hormone therapy, chemotherapy, and targeted therapy for breast cancer. *Proc. Sci.* **151**: 27–40.

28. Dickerson, E. B., Thomas, R., Fosmire, S. P., Lamerato-Kozicki, A. R., Bianco, S. R., Wojcieszyn, J. W., Breen, M., Helfand, S. C. and Modiano, J. F. 2005. Mutations of phosphatase and tensin homolog deleted from chromosome 10 in canine hemangiosarcoma. *Vet. Pathol.* **42**: 618–632.

29. Dickerson, E. B., Marley, K., Edris, W., Tyner, J. W., Schalk, V., MacDonald, V., Loriaux, M., Druker, B. J. and Helfand, S. C. 2013. Imatinib and dasatinib inhibit hemangiosarcoma and implicate PDGFR-β and Src in tumor growth. *Transl. Oncol.* **6**: 158–168.

30. Dobson, J. M., Samuel, S., Milstein, H., Rogers, K. and Wood, J. L. N. 2002. Canine neoplasia in the UK: Estimates of incidence rates from a population of insured dogs. *J. Small Anim. Pract.* **43**: 240–246.

31. Elders, R. C., Baines, S. J. and Catchpole, B. 2009. Susceptibility of the C2

canine mastocytoma cell line to the effects of tumor necrosis factor-related apoptosis-inducing ligand (TRAIL). *Vet. Immunol. Immunopathol.* **130**: 11–16.

32. Emery, J. G., Mcdonnell, P., Burke, M. B., Deen, K. C., Lyn, S., Silverman, C., Dul, E., Appelbaum, E. R., Eichman, C., Diprinzio, R., Dodds, R. A., James, I. E., Rosenberg, M., Lee, J. C. and Young, P. R. 1998. Osteoprotegerin is a receptor for the cytotoxic ligand TRAIL. *J. Biol. Chem.* **273**: 14363–14367.

33. Eustace, A. J., Conlon, N. T., McDermott, M. S. J., Browne, B. C., O'Leary, P., Holmes, F. A., Espina, V., Liotta, L. A., O'Shaughnessy, J., Gallagher, C., O'Driscoll, L., Rani, S., Madden, S. F., O'Brien, N. A., Ginther, C., Slamon, D., Walsh, N., Gallagher, W. M., Zagozdzon, R., Watson, W. R., O'Donovan, N. and Crown, J. 2018. Development of acquired resistance to lapatinib may sensitise HER2-positive breast cancer cells to apoptosis induction by obatoclax and TRAIL. *BMC Cancer*. **18**: 1–14.

34. Fei, H. rong, Yuan, C., Wang, G. ling, Zhao, Y., Li, Z. jun, Du, X. and Wang, F. Z. 2019. Caudatin potentiates the anti-tumor effects of TRAIL against human breast cancer by upregulating DR5. *Phytomedicine*. **62**: 1–9.

35. Finotello, R., Henriques, J., Sabattini, S., Stefanello, D., Felisberto, R., Pizzoni, S., Ferrari, R. and Marconato, L. 2017. A retrospective analysis of chemotherapy switch suggests improved outcome in surgically removed, biologically aggressive canine haemangiosarcoma. *Vet. Comp. Oncol.* **15**: 493–503.

36. Floros, T. and Tarhini, A. A. 2015. Anticancer cytokines: Biology and

clinical effects of interferon-α2, interleukin (IL)-2, IL-15, IL-21, and IL-12. *Semin. Oncol.* **42**: 539–548.

37. Fukumoto, S., Saida, K., Sakai, H., Ueno, H., Iwano, H. and Uchide, T. 2016. Therapeutic potential of endothelin inhibitors in canine hemangiosarcoma. *Life Sci.* **159**: 55–60.

38. Fyfe, G., Fisher, R., Rosenberg, S., Sznol, M., Parkinson, D. and Louie, A. 1995. Results of treatment of 255 patients with metastatic renal cell carcinoma who received high-dose recombinant interleukin-2 therapy. *J. Clin. Oncol.* **13**: 688–96.

39. Garden, O. A., Volk, S. W., Mason, N. J. and Perry, J. A. 2018. Companion animals in comparative oncology: One Medicine in action. *Vet. J.* **240**: 6–13.

40. GD, R. 2004. Mechanisms of bone metastasis. *N Engl j Med.* **350**: 1655–64.

41. Ghoncheh, M., Pournamdar, Z. and Salehiniya, H. 2016. Incidence and mortality and epidemiology of breast cancer in the world. *Asian Pacific J. Cancer Prev.* **17**: 43–46.

42. Goldschmidt, M. H., Peña, L., Rasotto, R. and Zappulli, V. 2011. Classification and grading of canine mammary tumors. *Vet. Pathol.* **48**: 117–131.

43. Göritz, M., Müller, K., Krastel, D., Staudacher, G., Schmidt, P., Kühn, M., Nickel, R. and Schoon, H. A. 2013. Canine splenic haemangiosarcoma: Influence of metastases, chemotherapy and growth pattern on post-splenectomy survival and expression of angiogenic factors. *J. Comp. Pathol.* **149**: 30–39.

44. Griffith, T. S., Chin, W. A., Jackson, G. C., Lynch, D. H. and Kubin, M. Z.

1998. Intracellular regulation of TRAIL-induced apoptosis in human melanoma cells. *J. Immunol.* **161**: 2833–2840.

45. Hansen, K. and Khanna, C. 2004. Spontaneous and genetically engineered animal models: Use in preclinical cancer drug development. *Eur. J. Cancer*. **40**: 858–880.

46. Hayes-Jordan, A. A., Ma, X., Menegaz, B. A., Lamhamedi-Cherradi, S. E., Kingsley, C. V., Benson, J. A., Camacho, P. E., Ludwig, J. A., Lockworth, C. R., Garcia, G. E. and Craig, S. L. 2018. Efficacy of ONC201 in desmoplastic small round cell tumor. *Neoplasia (United States)*. **20**: 524–532.

47. Head, K. ., Cullen, J. M., Dubielzig, R. R., Else, R. W., Misdorp, W., Patnaik, A. K., Tateyama, S. and Van der Gaag, I. 2003. Histological classification of tumors of the alimentary system of domestic animals, 2nd ed., Armed Forces institute of pathology, Washington.

48. Heishima, K., Mori, T., Ichikawa, Y., Sakai, H., Kuranaga, Y., Nakagawa, T., Tanaka, Y., Okamura, Y., Masuzawa, M., Sugito, N., Murakami, M., Yamada, N., Akao, Y. and Maruo, K. 2015. MicroRNA-214 and microRNA-126 are potential biomarkers for malignant endothelial proliferative diseases. *Int. J. Mol. Sci.* **16**: 25377–25391.

49. Heishima, K., Mori, T., Sakai, H., Sugito, N., Murakami, M., Yamada, N., Akao, Y. and Maruo, K. 2015. MicroRNA-214 promotes apoptosis in canine hemangiosarcoma by targeting the COP1-p53 axis. *PLoS One*. **10**: 1–19.

50. HellmÉn, E. 1992. Characterization of four in vitro established canine mammary carcinoma and one atypical benign mixed tumor cell lines. *Vitr. Cell. Dev. Biol. - Anim.* **28**: 309–319.

51. Hellmén, E., Moller, M., Blankenstein, M. A., Andersson, L. and Westermark, B. 2000. Expression of different phenotypes in cell lines from canine mammary spindle-cell tumours and osteosarcomas indicating a pluripotent mammary stem cell origin. *Breast Cancer Res. Treat.* **61**: 197–210.

52. Hurst, E. A., Pang, L. Y. and Argyle, D. J. 2019. The selective cyclooxygenase-2 inhibitor mavacoxib (Trocoxil) exerts anti-tumour effects in vitro independent of cyclooxygenase-2 expression levels. *Vet. Comp. Oncol.* **17**: 194–207.

53. Hymowitz, S. G., Connell, M. P. O., Ultsch, M. H., Hurst, A., Totpal, K., Ashkenazi, A., Vos, A. M. De, Kelley, R. F. and de Vos, A. M. 2000. A unique zinc-binding site revealed by a high-resolution X-ray structure of homotrimeric Apo2L/TRAIL. *Biochemistry*. **39**: 633–640.

54. Ichikawa, K., Liu, W., Zhao, L., Wang, Z., Liu, D., Ohtsuka, T., Zhang, H., Mountz, J. D., Koopman, W. J., Kimberly, R. P. and Zhou, T. 2001. Tumoricidal activity of a novel anti-human DR5 monoclonal antibody without hepatocyte cytotoxicity. *Nat. Med.* **7**: 954–960.

55. Johnson, A. S., Couto, C. G. and Weghorst, C. M. 1998. Mutation of the p53 tumor suppressor gene in spontaneously occurring osteosarcomas of the dog. *Carcinogenesis*. **19**: 213–217.

56. Johnson, K., Powers, B., Withrow, S., Sheetz, M., Curtis, C. and Wrigley, R. 1989. Splenomegaly in dogs. Predictors of neoplasia and survival after splenectomy. *J. Vet. Intern. Med.* **3**: 160–166.

57. Kelley, S. K., Harris, L. A., Xie, D., Deforge, L., Totpal, K., Bussiere, J. and

Fox, J. A. 2001. Preclinical studies to predict the disposition of Apo2L / tumor necrosis factor-related apoptosis-inducing ligand in humans: Characterization of in vivo efficacy , pharmacokinetics , and safety. *J. Pharmacol. Exp. Ther.* **299**: 31–38.

58. Khanna, C., Lindblad-Toh, K., Vali, D., London, C., Bergman, P., Barber, L., Matther, B., Kitchell, B., McNeil, E., Modiano, J., Niemi, S., Comstock, K. E., Ostrander, E., Westmoreland, S. and Withrow, S. 2006. The dog as a cancer model. *Nat. Biotechnol.* **24**: 1065–1066.

59. Khemlina, G., Ikeda, S. and Kurzrock, R. 2017. The biology of hepatocellular carcinoma: implications for genomic and immune therapies. *Mol. Cancer*. **16**: 1–10.

60. Kim, J.-H., Graef, A., Dickerson, E. and Modiano, J. 2015. Pathobiology of hemangiosarcoma in dogs: Research advances and future perspectives. *Vet. Sci.* **2**: 388–405.

61. Kischkel, F. C., Lawrence, D. A., Chuntharapai, A., Schow, P., Kim, K. J. and Ashkenazi, A. 2000. Apo2L/TRAIL-dependent recruitment of endogenous FADD and caspase-8 to death receptors 4 and 5. *Immunity*. **12**: 611–620.

62. Kischkel, F. C., Lawrence, D. A., Tinel, A., LeBlanc, H., Virmani, A., Schow, P., Gazdar, A., Blenis, J., Arnott, D. and Ashkenazi, A. 2001. Death receptor recruitment of endogenous caspase-10 and apoptosis initiation in the absence of caspase-8. *J. Biol. Chem.* **276**: 46639–46646.

63. Kleine, L., Zook, B. and Munson, T. 1970. Primary cardiac hemangiosarcoma in dogs. *J Am Vet Med Assoc*. **157**: 326–337.

64. Kodama, A., Sakai, H., Matsuura, S., Murakami, M., Murai, A., Mori, T., Maruo, K., Kimura, T., Masegi, T. and Yanai, T. 2009. Establishment of canine hemangiosarcoma xenograft models expressing endothelial growth factors, their receptors, and angiogenesis-associated homeobox genes. *BMC Cancer*. **9**: 363.

65. Konecny, G. E., Pegram, M. D., Venkatesan, N., Finn, R., Yang, G., Rahmeh, M., Untch, M., Rusnak, D. W., Spehar, G., Mullin, R. J., Keith, B. R., Gilmer, T. M., Berger, M., Podratz, K. C. and Slamon, D. J. 2006. Activity of the dual kinase inhibitor lapatinib (GW572016) against HER-2-overexpressing and trastuzumab-treated breast cancer cells. *Cancer Res.* **66**: 1630–1639.

66. Koornstra, J. J., Kleibeuker, J. H., van Geelen, C. M. M., Rijcken, F. E. M., Hollema, H., de Vries, E. G. E. and de Jong, S. 2003. Expression of TRAIL (TNF-related apoptosis-inducing ligand) and its receptors in normal colonic mucosa, adenomas, and carcinomas. *J. Pathol.* **200**: 327–335.

67. Koshino, A., Goto-Koshino, Y., Setoguchi, A., Ohno, K. and Tsujimoto, H. 2016. Mutation of p53 gene and its correlation with the clinical outcome in dogs with lymphoma. *J. Vet. Intern. Med.* **30**: 223–229.

68. Laia Solano-Gallego, C. M. 2016. Reproductive system. p. 319. *In*: *canine an d feline cytology a color atras and interpretation guide*, 3rd ed., (Rose E. Raskin, Denny J. Meyer eds.) Elsevier, St.Louis, Missouri.

69. Lauwes, G. ., Carneiro, F., Graham, D., Curado, M. P., Franceshi, S., Montgomery, E., Tatematsu, M. and Hattori, T. 2010. Tumors of the stomach. pp. 48–58. *In*: *WHO Classification of Tumours of the Digestive*

System, 4th ed., (Bosman, Fred T., Carneiro, Fatima, Hruban, Ralph H. and Theise, Neil D. eds.) International Agency for Research on Cancer, Lyon.

70. LeBlanc, H. N. and Ashkenazi, A. 2003. Apo2L/TRAIL and its death and decoy receptors. *Cell Death Differ.* **10**: 66–75.

71. Lee, S. and Margolin, K. 2011. Cytokines in cancer immunotherapy. *Cancers (Basel).* **3**: 3856–3893.

72. Leeuwen, I. S. Van, Hellmèn, E., Cornelisse, C. J., Burgh, B. D. Van and Rutteman, G. R. 1996. P53 mutations in mammary tumor cell lines and corresponding tumor tissues in the dog. *Anticancer Res.* **16**: 3737–3744.

73. Leyva, F. J., Loughin, C. A., Dewey, C. W., Marino, D. J., Akerman, M. and Lesser, M. L. 2018. Histopathologic characteristics of biopsies from dogs undergoing surgery with concurrent gross splenic and hepatic masses: 125 cases (2012-2016). *BMC Res. Notes*. **11**: 14–18.

74. Liptak, J. M., Dernell, W. S., Monnet, E., Powers, B. E., Bachand, A. M., Kenney, J. G. and Withrow, S. J. 2004. Massive hepatocellular carcinoma in dogs: 48 cases (1992-2002). *J Am Vet Med Assoc*. **225**: 1225–1230.

75. Lodish, H., Berk, A., Kaiser, C. A., Krieger, M., Bretscher, A., Plogh, H., Amon, A. and Scott, M. P. 2013. Molecular cell biology. pp. 65–66. *In*: *Molecular cell Biology*, 7th ed., W. H. Freeman and company, New York.

76. Marconato, L., Romaneli, G., Stefanello, D., Giacoboni, C., Bonfanti, U., Bettini, G., Finotello, R., Verganti, S., Valenti, P., Ciaramella, L. and Zini, E. 2009. Prognostic factors for dogs with mammary inflammatory carcinoma: 43 cases (2003-2008). *J Am Vet Med Assoc*. **235**: 967–972.

77. Marsters, S. A., Sheridan, J. P., Pitti, R. M., Huang, A., Skubatch, M., Baldwin, D., Yuan, J., Gurney, A., Goddard, A. D., Godowski, P. and Ashkenazi, A. 1997. A novel receptor for Apo2L / TRAIL contains a truncated death domain. *Curr. Biol.* **7**: 1003–1006.

78. Martín-Ruiz, A., Peña, L., González-Gil, A., Díez-Córdova, L. T., Cáceres, S. and Illera, J. C. 2018. Effects of indole-3-carbinol on steroid hormone profile and tumor progression in a mice model of canine inflammatory mammarycancer. *BMC Cancer*. **18**: 10–14.

79. Matsuyama, A., Poirier, V. J., Mantovani, F., Foster, R. A. and Mutsaers, A. J. 2017. Adjuvant doxorubicin with or without metronomic cyclophosphamide for canine splenic hemangiosarcoma. *J. Am. Anim. Hosp. Assoc.* **53**: 304–312.

80. Mayr, B., Schaffner, W., Botto, I., Reifinger, M. and Loupal, G. 1997. Canine tumor suppressor gene p53-mutation in a case of adenoma of circumanal glands. *Vet. Res. Commun.* **21**: 369–373.

81. Huarte, E., Fisher, J., Turk, M. J., Mellinger, D., Foster, C., Wolf, B., Meehan, K. R., Fadul, C. E. and Ernstoff, M. S. 2009. Ex vivo expansion of tumor specific lymphocytes with IL-15 and IL-21 for adoptive immunotherapy in melanoma. *Cancer Lett.* **285**: 80–88.

82. Menezes, M. E., Genetics, M., Bhatia, S., Genetics, M., Bhoopathi, P., Genetics, M., Das, S. K., Genetics, M., Emdad, L., Genetics, M., Dasgupta, S., Genetics, M., Dent, P., Wang, X. and Genetics, M. 2014. MDA-7/IL-24: Multifunctional cancer killing cytokine. *Adv Exp Med Biol*. **818**: 127–153.

83. Michael H. Goldschmidt, Laura Pena, V. zappulli 2017. Tumors of the

mammary gland. p. 723. *In*: *Tumors in Domestic Animals*, Fifth ed., (Meuten, Donald J. eds.) Wiley Blackwell, Ames.

84. Monzur Rahman, Sean R. Davis,Janet G. Pumphrey,Jing Bao,Marion M. Nau,Paul S. Meltzer, S. L. 2009. TRAIL induces apoptosis in triple-negative breast cancer cells with a mesenchymal phenotype. *Breast Cancer Res. Treat.* **113**: 217–230.

85. Murai, A., Asa, S. A., Kodama, A., Hirata, A., Yanai, T. and Sakai, H. 2012. Constitutive phosphorylation of the mTORC2/Akt/4E-BP1 pathway in newly derived canine hemangiosarcoma cell lines. *BMC Vet. Res.* **8**: 1–14.

86. Murakami, M., Sakai, H., Kodama, A., Mori, T., Maruo, K., Yanai, T. and Masegi, T. 2008. Expression of the anti-apoptotic factors Bcl-2 and survivin in canine vascular tumours. *J. Comp. Pathol.* **139**: 1–7.

87. Murakami, M., Sakai, H., Kodama, A., Yanai, T., Mori, T., Maruo, K. and Masegi, T. 2009. Activation of matris metalloproteinase (MMP)-2 by membrane type 1-MMP and abnormal immunolocalization of the basement membrane components laminin and type Ⅳ collagen in canine spontaneous hemangiosarcoma. *Histol. Histopathol.* **24**: 437–446.

88. Muto, T., Wakui, S., Takahashi, H., Maekawa, S., Masaoka, T., Ushigome, S. and Furusato, M. 2000. P53 gene mutations occurring in spontaneous benign and malignant mammary tumors of the dog. *Vet. Pathol.* **37**: 248–253.

89. Naoum, G. E., Buchsbaum, D. J., Tawadros, F., Farooqi, A. and Arafat, W. O. 2017. Journey of TRAIL from bench to bedside and its potential role in immuno-oncology. *Oncol. Rev.* **11**: 26–42.

90. Nóbrega, D. F., Sehaber, V. F., Madureira, R. and Bracarense, A. P. F. R. L. 2019. Canine cutaneous haemangiosarcoma: Biomarkers and survival. *J. Comp. Pathol.* **166**: 87–96.

91. Okano, H., Shiraki, K., Inoue, H., Kawakita, T., Yamanaka, T., Deguchi, M., Sugimoto, K., Sakai, T., Ohmori, S., Fujikawa, K., Murata, K. and Nakano, T. 2003. Cellular FLICE/caspase-8-inhibitory protein as a principal regulator of cell death and survival in human hepatocellular carcinoma. *Lab. Investig.* **83**: 1033–1043.

92. Olsen, J. A., Thomson, M., O'Connell, K. and Wyatt, K. 2018. Combination vinblastine, prednisolone and toceranib phosphate for treatment of grade II and III mast cell tumours in dogs. *Vet. Med. Sci.* **4**: 237–251.

93. Palacios, C., Yerbes, R. and López-Rivas, A. 2006. Flavopiridol induces cellular FLICE-inhibitory protein degradation by the proteasome and promotes TRAIL-induced early signaling and apoptosis in breast tumor cells. *Cancer Res.* **66**: 8858–8869.

94. Pan, G., Ni, J., Wei, Y. F., Yu, G. I., Gentz, R. and Dixit, V. M. 1997. An antagonist decoy receptor and a death domain-containing receptor for TRAIL. *Science (80-.).* **277**: 815–818.

95. Pan, G., O'Rourke, K., Chinnaiyan, A. M., Gentz, R., Ebner, R., Ni, J. and Dixit, V. M. 1997. The receptor for the cytotoxic ligand TRAIL. *Science (80-.).* **276**: 111–113.

96. Paoloni, M. C. and Khanna, C. 2007. Comparative oncology today. *Vet Clin North Am Small anim Pr.* **37**: 1023–v.

97. Pawlak A, DE Miguel D, Kutkowska J, Obmińska-Mrukowicz B, Rapak A,

M.-L. L. 2017. Flavopiridol strongly sensitizes canine lymphoma cells to TRAIL-induced apoptosis. *Anticancer Res.* **37**: 6655–6665.

98. Perez, A. M. D., Tabanera, E. and Pena, L. 2001. Inflammatory mammary carcinoma in dogs: 33 case (1995-1999). *J Am Vet Med Assoc.* **219**: 1110–1114.

99. Philibert, J. C., Snyder, P. W., Glickman, N., Glickman, L. T., Knapp, D. W. and Waters, D. J. 2003. Influence of host factors on survival in dogs with malignant mammary gland tumors. *J. Vet. Intern. Med.* **17**: 102–106.

100. Pinho, S. S., Carvalho, S., Cabral, J., Reis, C. A. and Gärtner, F. 2012. Canine tumors: A spontaneous animal model of human carcinogenesis. *Transl. Res.* **159**: 165–172.

101. Pitti, R. M., Marsters, S. A., Ruppert, S., Donahue, C. J., Moore, A. and Ashkenazi, A. 1996. Induction of apoptosis by Apo-2 ligand, a new member of the tumor necrosis factor cytokine family. *J. Biol. Chem.* **271**: 12687–12690.

102. Premzl, M. 2016. Comparative genomic analysis of eutherian tumor necrosis factor ligand genes. *Immunogenetics.* **68**: 125–132.

103. Prymak C, McKee LJ, Goldschmidt MH, G. L. 1988. Epidemiologic, clinical, pathologic, and prognostic characteristics of splenic hemangiosarcoma and splenic hematoma in dogs: 217 cases (1985). *J Am Vet Med Assoc.* **193**: 706–12.

104. PT Daniel, T wieder, I Sturm, K. S.-O. 2001. The kiss of death: Promises and failures of death receptors and ligands in cancer therapy. *Leukemia.* **15**: 1022–1032.

105. Pukae, L., Kanakaraj, P., Humphreys, R., Alderson, R., Bloom, M., Sung, C., Riccobene, T., Johnson, R., Fiscella, M., Mahoney, A., Carrell, J., Boyd, E., Yao, X. T., Zhang, L., Zhong, L., Von Kerczek, A., Shepard, L., Vaughan, T., Edwards, B., Dobson, C., Salcedo, T. and Albert, V. 2005. HGS-ETR1, a fully human TRAIL-receptor 1 monoclonal antibody, induces cell death in multiple tumour types in vitro and in vivo. *Br. J. Cancer*. **92**: 1430–1441.

106. Queiroga, F. L., Raposo, T., Carvalho, M. I., Prada, J. and Pires, I. 2011. Canine mammary tumours as a model study human breast cancer: most recent findings. *In Vivo (Brooklyn).* **25**: 455–465.

107. Rasotto, R., Zappulli, V., Castagnaro, M. and Goldschmidt, M. H. 2012. A retrospective study of those histopathologic parameters predictive of invasion of the lymphatic system by canine mammary carcinomas. *Vet. Pathol.* **49**: 330–340.

108. Rasotto, R., Berlato, D., Goldschmidt, M. H. and Zappulli, V. 2017. Prognostic significance of canine mammary tumor histologic subtypes: An observational cohort study of 229 cases. *Vet. Pathol.* **54**: 571–578.

109. Finotello, R., Stefanello,D., Zini, E. and Marconato, L. 2017. Comparison of doxorubicin-cyclophosphamide with doxorubicin-dacarbazine for the adjuvant treatment of canine hemangiosarcoma. *Vet. Comp. Oncol.* **15**: 25–35.

110. Rong, S., Cai, J. H. and Andrews, J. 2008. Cloning and apoptosis-inducing activities of canine and feline TRAIL. *Mol. Cancer Ther.* **7**: 2181–2191.

111. Rossi, F., Sabattini, S., Vascellari, M. and Marconato, L. 2018. The impact of toceranib, piroxicam and thalidomide with or without hypofractionated

radiation therapy on clinical outcome in dogs with inflammatory mammary carcinoma. *Vet. Comp. Oncol.* **16**: 497–504.

112. Rytomaa Marjatta, Martins L. Miguel, D. J. 1999. Involvement of FADD and caspase-8 signalling in detachment-induced apoptosis. *Curr. Biol.* **9**: 1043–1046.

113. Sato, M., Kanemoto, H., Kagawa, Y., Kobayashi, T., Goto-Koshino, Y., Mochizuki, H., Takahashi, M., Fujino, Y., Ohno, K. and Tsujimoto, H. 2012. Evaluation of the prognostic significance of BCL6 gene expression in canine high-grade B-cell lymphoma. *Vet. J.* **191**: 108–114.

114. Schiffman, J. D. and Breen, M. 2015. Comparative oncology: what dogs and other species can teach us about humans with cancer. *Philos. Trans. R. Soc. B Biol. Sci.* **370**: 1–13.

115. Schneider, P., Bodmer, J. L., Thome, M., Hofmann, K., Holler, N. and Tschopp, J. 1997. Characterization of two receptors for TRAIL. *FEBS Lett.* **416**: 329–334.

116. Schultheiss, P. C. 2004. A retrospective study of visceral and nonvisceral HSA and hemangiomas in domestic animals. *J. Vet. Diagnostic Investig.* **16**: 522–526.

117. Sheridan, J. P., Marsters, S. A., Pitti, R. M., Gurney, A., Skubatch, M., Baldwin, D., Ramakrishnan, L., Gray, C. L., Baker, K., Wood, W. I., Goddard, A. D., Godowski, P. and Ashkenazi, A. 1997. Control of TRAIL-induced apoptosis by a family of signaling and decoy receptors. *Science.* **277**: 818–821.

118. Simonet, W. ., Lacey, D. ., Dunstan, C. ., Kelley, M., Chang, M.-S., Lüthy,

R., Nguyen, H. ., Wooden, S., Bennett, L., Boone, T., Shimamoto, G., DeRose, M., Elliott, R., Colombero, A., Tan, H.-L., Trail, G., Sullivan, J., Davy, E., Bucay, N., Renshaw-Gegg, L., Hughes, T. ., Hill, D., Pattison, W., Campbell, P., Sander, S., Van, G., Tarpley, J., Derby, P., Lee, R. and Boyle, W. . 1997. Osteoprotegerin: A novel secreted protein involved in the regulation of bone density. *Cell*. **89**: 309–319.

119. Singh, T. R., Shankar, S. and Srivastava, R. K. 2005. HDAC inhibitors enhance the apoptosis-inducing potential of TRAIL in breast carcinoma. *Oncogene*. **24**: 4609–4623.

120. Solomon, B. J., Besse, B., Bauer, T. M., Felip, E., Soo, R. A., Camidge, D. R., Chiari, R., Bearz, A., Lin, C., Gadgeel, S. M., Riely, G. J., Tan, E. H., Seto, T., James, L. P., Clancy, J. S., Abbattista, A., Martini, J., Chen, J., Peltz, G. and Thurm, H. 2018. Lorlatinib in patients with ALK-positive non-small-cell lung cancer: results from a global phase 2 study. *Lancet Oncol.* **19**: 1654–1667.

121. Sorenmo, K. U., Worley, D. R. and Goldschmidt, M. H. 2013. Tumors of the Mammary Gland. pp. 538–547. *In*: *Withrow and Masewen's small animal clinical oncology*, 5th ed., (Withrow, Stephen J., Vail, David M. and Page, Rodney L. eds.) Elsevier saunders, St.Louis.

122. Spangler WL, C. M. 1992. Prevalence, type, and importance of splenic diseases in dogs: 1,480 cases (1985-1989). *J Am Vet Med Assoc.* **200**: 829–34.

123. Spee, B., Jonkers, M. D. B., Arends, B., Rutteman, G. R., Rothuizen, J. and Penning, L. C. 2006. Specific down-regulation of XIAP with RNA

interference enhances the sensitivity of canine tumor cell-lines to TRAIL and doxorubicin. *Mol. Cancer*. **5**: 1–10.

124. Sprick, M. R., Weigand, M. A., Rieser, E., Rauch, C. T., Juo, P., Blenis, J., Krammer, P. H. and Walczak, H. 2000. FADD/MORT1 and caspase-8 are recruited to TRAIL receptors 1 and 2 and are essential for apoptosis mediated by TRAIL receptor 2. *Immunity*. **12**: 599–609.

125. Srivastava, R. K., Kurzrock, R. and Shankar, S. 2010. MS-275 sensitizes TRAIL-resistant breast cancer cells, inhibits angiogenesis and metastasis, and reverses epithelial-mesenchymal transition in vivo. *Mol. Cancer Ther.* **9**: 3254–3266.

126. Stephan, L. and Jermy, B. 1994. Principles of bioinorganic chemistry, 1st ed., pp.44-46. Unicersity Science Books, California.

127. Stoklasek, T. A., Schluns, K. S. and Lefrançois, L. 2006. Combined IL-15/IL-15Rα immunotherapy maximizes IL-15 activity in vivo. *J. Immunol.* **177**: 6072–6080.

128. Szczubiał, M. and Łopuszynski, W. 2011. Prognostic value of regional lymph node status in canine mammary carcinomas. *Vet. Comp. Oncol.* **9**: 296–303.

129. Takeda, K., Stagg, J., Yagita, H., Okumura, K. and Smyth, M. J. 2007. Targeting death-inducing receptors in cancer therapy. *Oncogene*. **26**: 3745–3757.

130. Tamura, D., Saito, T., Murata, K., Kawashima, M. and Asano, R. 2015. Celecoxib exerts antitumor effects in canine mammary tumor cells via COX-2-independent mechanisms. *Int. J. Oncol.* **46**: 1393–1404.

131. Tolcher, A. W., Mita, M., Meropol, N. J., Von Mehren, M., Patnaik, A., Padavic, K., Hill, M., Mays, T., McCoy, T., Fox, N. L., Halpern, W., Corey, A. and Cohen, R. B. 2007. Phase I pharmacokinetic and biologic correlative study of mapatumumab, a fully human monoclonal antibody with agonist activity to tumor necrosis factor-related apoptosis-inducing ligand receptor-1. *J. Clin. Oncol.* **25**: 1390–1395.

132. Tran, C. M., Moore, A. S. and Frimberger, A. E. 2016. Surgical treatment of mammary carcinomas in dogs with or without postoperative chemotherapy. *Vet. Comp. Oncol.* **14**: 252–262.

133. Trarbach, T., Moehler, M., Heinemann, V., Köhne, C. H., Przyborek, M., Schulz, C., Sneller, V., Gallant, G. and Kanzler, S. 2010. Phase II trial of mapatumumab, a fully human agonistic monoclonal antibody that targets and activates the tumour necrosis factor apoptosis-inducing ligand receptor-1 (TRAIL-R1), in patients with refractory colorectal cancer. *Br. J. Cancer*. **102**: 506–512.

134. Trivedi, R. and Mishra, D. P. 2015. Trailing TRAIL resistance: Novel targets for TRAIL sensitization in cancer cells. *Front. Oncol.* **5**: 1–20.

135. Valli VE, Bienzle D, Meuten DJ, L. K. 2017. Tumors of hemolymphatic system. pp. 309–313. *In*: *Tumor in Domestinc Animals*, 5th ed., (DJ, Meuten eds.) Wiley Blackwell, Ames.

136. Veldhoen, N., Stewart, J., Brown, R. and Milner, J. 1998. Mutations of the p53 gene in canine lymphoma and evidence for germ line p53 mutations in the dog. *Oncogene*. **16**: 249–255.

137. Vousden, K. H. and Lu, X. 2002. Live or let die: The cell's response to p53.

Nat. Rev. Cancer. **2**: 594–604.

138. Walczak, H., Miller, R. E., Ariail, K., Gliniak, B., Griffith, T. S., Kubin, M., Chin, W., Jones, J., Woodward, A., Le, T., Smith, C., Smolak, P., Goodwin, R. G., Rauch, C. T., Schuh, J. C. and Lynch, D. H. 1999. Tumoricidal activity of tumor necrosis factor-related apoptosis-inducing ligand in vivo. *Nat. Med.* **5**: 157–163.

139. Walczak, H., Degli-esposti, M. A., Johnson, R. S., Smolak, P. J., Waugh, J. Y., Boiani, N., Timour, M. S., Gerhart, M. J., Schooley, K. A., Smith, C. A., Goodwin, R. G. and Rauch, C. T. 1997. TRAIL-R2: a novel apoptosis-mediating receptor for TRAIL. *EMBO J.* **16**: 5386–5397.

140. Wang, X., Simpson, E. R. and Brown, K. A. 2015. p53: Protection against tumor growth beyond effects on cell cycle and apoptosis. *Cancer Res.* **75**: 5001–5007.

141. Wawryk-Gawda, E., Chylińska-Wrzos, P., Lis-Sochocka, M., Chłapek, K., Bulak, K., Jędrych, M. and Jodłowska-Jędrych, B. 2014. P53 protein in proliferation, repair and apoptosis of cells. *Protoplasma*. **251**: 525–533.

142. Wiley, S. R., Schooley, K., Smolak, P. J., Din, W. S., Huang, C. P., Nicholl, J. K., Sutherland, G. R., Smith, T. D., Rauch, C., Smith, C. A. and Goodwin, R. G. 1995. Identification and characterization of a new member of the TNF family that induces apoptosis. *Immunity*. **3**: 673–82.

143. Xu, W., Jones, M. onica, Liu, B., Zhu, X., Johnson, C. B., Edwards, A. C., Kong, L., Jeng, E. K., Han, K., Marcus, W. D., Rubinstein, M. P., Rhode, P. R. and Wong, H. C. 2013. Efficacy and mechanism-of-action of a novel superagonist interleukin-15: interleukin-15 receptor αSu/Fc fusion complex

in syngeneic murine models of multiple myeloma. *Cancer Res.* **73**: 3075–3086.

144. Yonemaru, K., Sakai, H., Murakami, M., Kodama, A., Mori, T., Yanai, T., Maruo, K. and Masegi, T. 2007. The significance of p53 and retinoblastoma pathways in canine hemangiosarcoma. *J. Vet. Med. Sci.* **69**: 271–278.
145. Yonemaru, K., Sakai, H., Murakami, M., Yanai, T. and Masegi, T. 2006. Expression of vascular endothelial growth factor, basic fibroblast growth factor, and their receptors (Flt-1, Flk-1, and Flg-1) in canine vascular tumors. *Vet Pathol.* **980**: 971–980.
146. Zandvliet, M. 2016. Canine lymphoma: a review. *Vet. Q.* **36**: 76–104.
147. Zhang, H., Pei, S., Zhou, B., Wang, H., Du, H., Zhang, D. and Lin, D. 2018. Establishment and characterization of a new triple-negative canine mammary cancer cell line. *Tissue Cell.* **54**: 10–19.
148. Zhang, L. and Fang, B. 2005. Mechanisms of resistance to TRAIL-induced apoptosis in cancer. *Cancer Gene Ther.* **12**: 228–237.